

The Physicochemical Hydrodynamics of Vascular Plants

Abraham D. Stroock,¹ Vinay V. Pagay,²
Maciej A. Zwieniecki,³ and N. Michele Holbrook⁴

¹School of Chemical and Biomolecular Engineering and Kavli Institute at Cornell for Nanoscale Science, Cornell University, Ithaca, New York 14853; email: ads10@cornell.edu

²Department of Horticulture, Cornell University, Ithaca, New York 14853; email: vvp4@cornell.edu

³Department of Plant Sciences, University of California, Davis, California 95616; email: mzwienie@ucdavis.edu

⁴Department of Organismic and Evolutionary Biology, Harvard University, Cambridge, Massachusetts 02138; email: holbrook@fas.harvard.edu

Annu. Rev. Fluid Mech. 2014. 46:615–42

First published online as a Review in Advance on October 9, 2013

The *Annual Review of Fluid Mechanics* is online at fluid.annualreviews.org

This article's doi:
10.1146/annurev-fluid-010313-141411

Copyright © 2014 by Annual Reviews.
All rights reserved

Keywords

xylem, transpiration, cavitation, membrane, osmosis

Abstract

Plants live dangerously, but gracefully. To remain hydrated, they exploit liquid water in the thermodynamically metastable state of negative pressure, similar to a rope under tension. This tension allows them to pull water out of the soil and up to their leaves. When this liquid rope breaks, owing to cavitation, they catch the ends to keep it from unraveling and then bind it back together. In parallel, they operate a second vascular system for the circulation of metabolites through their tissues, this time with positive pressures and flow that passes from leaf to root. In this article, we review the current state of understanding of water management in plants with an emphasis on the rich coupling of transport phenomena, thermodynamics, and active biological processes. We discuss efforts to replicate plant function in synthetic systems and point to opportunities for physical scientists and engineers to benefit from and contribute to the study of plants.

Xylem: the nonliving vascular conduits of plants that transport water during transpiration

Phloem: the vascular conduits that transport sugars produced by photosynthesis in leaves to other tissues in the plant

Cavitation the nucleation and growth of a bubble filled with gas and vapor within a liquid due to supersaturation and superheat

1. INTRODUCTION

Green plants are machines that run on sunlight, carbon dioxide, and water. Harvesting these ingredients from their environment poses multiple challenges of mass transfer. First, plants must grow into extended, multicellular organisms to reach for the sky to capture sunlight and exchange carbon dioxide and oxygen with the atmosphere. The photosynthetic reaction itself consumes water ($\text{light} + 6\text{H}_2\text{O} + 6\text{CO}_2 \rightarrow \text{C}_6\text{H}_{12}\text{O}_6 + 6\text{O}_2$), and worse, exposure to air leads to evaporation. Second, plants generate all of the photosynthetic products in their leaves, and they must export these products to the rest of their tissues for growth and storage. As with other multicellular organisms, they have evolved vascular structure to allow for efficient convective transport over long distances (**Figure 1**). In contrast with other large life-forms such as mammals, plants exploit almost entirely passive means to drive fluids through their veins. Rather than dedicate biochemical energy to pumping, they couple to the ambient gradient in the water saturation between the soil and the atmosphere to drive flow up through their xylem, and they capture the inevitable gradients of osmolarity generated by the localized synthesis of sugar to drive flow back down through their phloem (**Figure 1**).

These processes sound simple, yet they involve unusual manipulations of the liquid state and a degree of process integration (across scales and physical, chemical, and biological functions) that we have yet to achieve in human technologies. In **Figure 2**, measurements of the pressure within the terminal xylem vessels illustrate an extraordinary consequence of plants' strategy for moving liquid up to their leaves (Scholander et al. 1965): In all species represented, the pressures are negative; the liquid is under tension. This metastable state is a form of superheat in which the liquid is prone to cavitation (boiling). Management of this fragile state plays a central role in defining the physiology and function of vascular plants. The histological sections in **Figure 1** provide a sense of the architectural complexity that allows for the coordination of these transport processes with a vast diversity of other biological activities.

In this review, we aim to provide a translation for physical scientists of the insights that plant scientists have gained over the past century into the structure and function of plant vasculature. We emphasize the concepts of physicochemical hydrodynamics: the coupling of transport phenomena, thermodynamics, and kinetics (Levich 1962). For a focus on mechanics and control, we point the reader to Rand's (1983) review in this journal. For coverage of these topics aimed at plant scientists, we suggest Nobel's (1999) book and a volume edited by two of us (Holbrook & Zwieniecki 2005). We start with a minimalist overview of the relevant plant physiology (Section 2) before moving to a presentation of the current theoretical and experimental understanding of transport in the xylem and phloem (Sections 3 and 4). In Sections 5 and 6, we discuss active areas of research related to recovery after cavitation and the roles played by vascular function in defining plant morphology. Section 7 presents a review of efforts to capture the vascular function of plants in synthetic systems. We end in Section 8 with a discussion of outstanding questions and opportunities.

2. VASCULAR PHYSIOLOGY OF PLANTS

In this section, we provide an overview of the relevant physiological components using **Figures 1** and **3**, without discussing transport processes in detail. In Section 3, we call on these components as we review the transport phenomena.

2.1. The Pipes

The micrographs in **Figure 1** show the typical distribution of the xylem and phloem capillaries within the tissue. Their internal diameters range from 10 to 500 μm , depending on the location

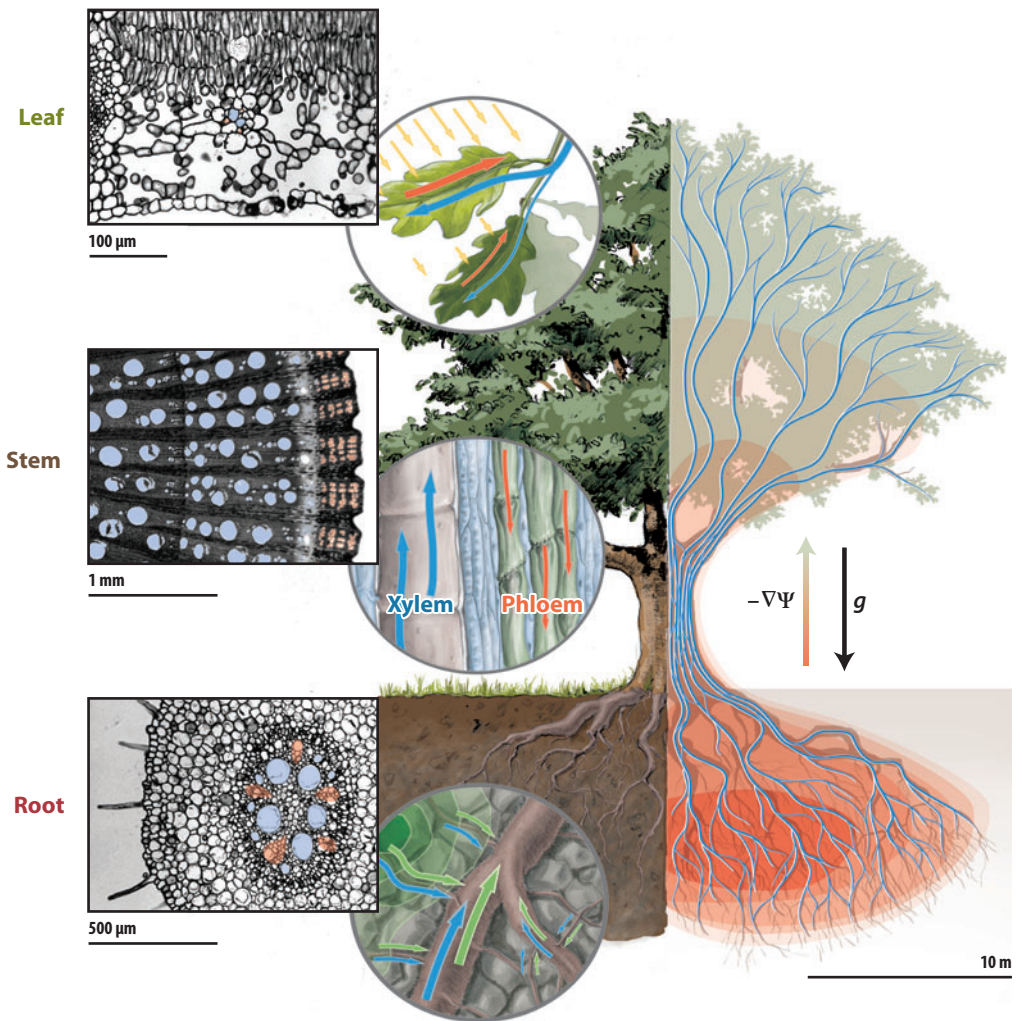


Figure 1

Global view of transport processes in a vascular plant. The xylem mediates the net transfer of water from the soil to the atmosphere down a gradient in water potential, $\nabla\Psi_w$ (Pa m^{-1}). The phloem carries a flow of sugars and other metabolites down the plant from the leaves to the tissues. Optical micrographs show cross sections of a leaf, stem, and root with the approximate location of the xylem (blue) and phloem (orange). Micrograph of a leaf courtesy of Martin Goffinet. The background drawing of a tree courtesy of the STEP research group (ETH Zürich).

within the plant and the species (Tyree & Zimmermann 2002). Xylem conduits are formed from the interconnected, hollow walls of dead cells. The phloem sieve tubes are formed of the interconnected internal volumes (cytosols) of living cells.

2.2. The Membranes

The transfer between multiple phases—gas, pure liquid, solutions, hydrated matrices—implicated in the function of the xylem and phloem requires that the internal phases be coupled to each

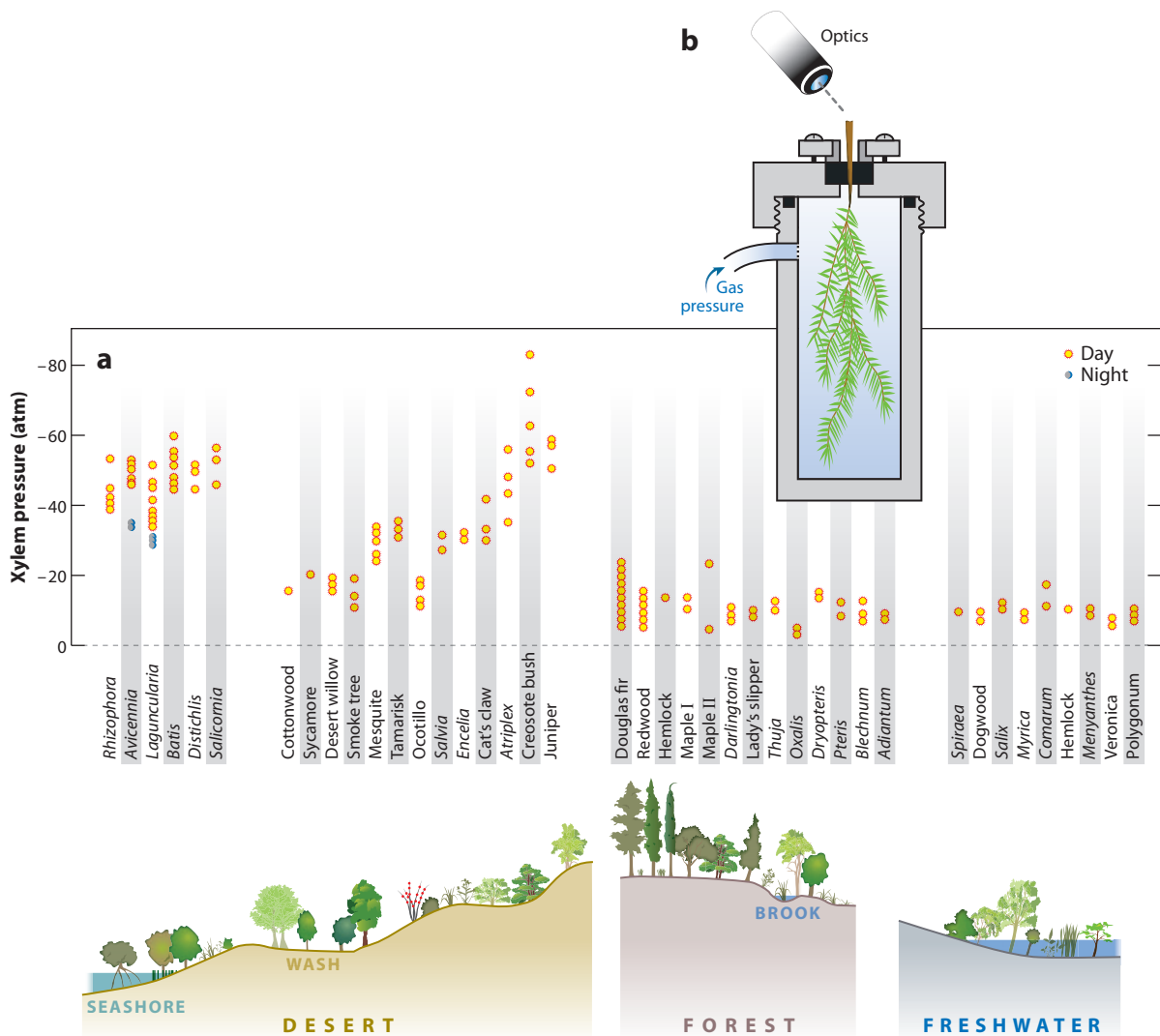


Figure 2

Pressure in the xylem. (a) The pressure relative to atmospheric pressure in leaves and needles ($P_{X,L} - P_0$) is reported in atmospheres (~ 0.1 MPa) for a variety of species in a variety of climates. The values are negative. (b) Schematic depiction of the Scholander leaf pressure chamber. A cut leaf or terminal shoot is placed in the chamber with its stem exposed through a seal. The air pressure is raised within the chamber until a droplet of liquid is observed optically at the cut surface of the stem. This positive balance pressure is taken as an estimate of the negative pressure in the xylem before excision. This method has been shown to agree with more direct, mechanical measurements (Holbrook et al. 1995, Melcher et al. 1998). Figure adapted from Scholander et al. (1965).

other and to external phases via membranes (Figure 3). We use the term membrane in the physical sense of a permeable or semipermeable material that separates two volumes of fluid. In biology, the term membrane refers specifically to the lipid bilayer that surrounds living cells and intracellular compartments. Figure 3 presents a highly simplified depiction of the structure and arrangement of these membranes in the leaf, stem, and root. These membranes allow for the

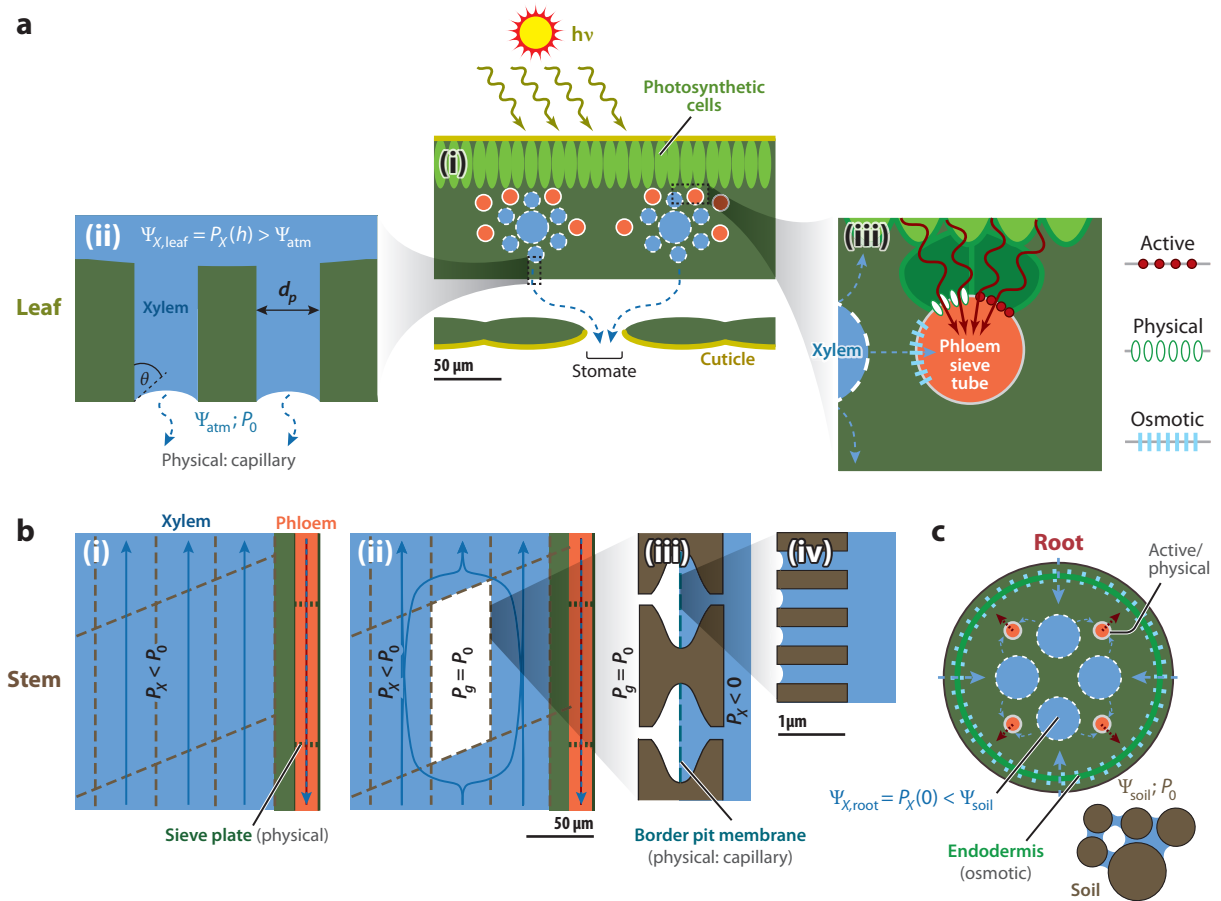


Figure 3

Schematic representations of the membranes that mediate transport processes in plants. (a) The xylem (blue) delivers water to the leaf; the phloem (orange) exports sugars formed by photosynthesis from the leaf. (i) The principal flow of water during transpiration goes to evaporation through stomata on the underside of the leaf. (ii) Evaporation occurs through a physical membrane that can be represented as a wettable porous material. The embolized vessel lumen pressure, P_g , rises to P_0 . (iii) Sugars diffuse or are pumped into the phloem sieve tubes (dark red arrows) through physical (plasmodesmata) and active membranes; water is drawn in from the xylem (blue dashed line) through an osmotic membrane. Water also goes to photosynthesis (up) and evaporation (down). (b,i) In the stem, water flows up in the xylem (blue arrow) and aqueous solutions flow down in the phloem (red-blue dashed arrow). The conduits in both the xylem and phloem are segmented by physical membranes. In the phloem, these are called sieve plates. (ii) The pressure in the xylem, P_X , is lower than atmospheric pressure, P_0 , such that cavitation can occur. The porous vessel walls can stop the spread of a gas bubble (white) and allow flow to take alternate paths around the emptied segment. (iii,iv) The pores (bordered pits) connecting adjacent segments in the xylem pass through the vessel walls. They are bifurcated by thin physical membranes (bordered pit membranes). When wetted on both sides, the bordered pit membrane passes liquid flow; when dried on one side, its small pores can sustain a pressure difference by capillarity (iv). (c) In the root, reduced pressure in the xylem drives the flow of water from the soil through the endodermis, an osmotic membrane. Solutes pass from the phloem into the tissue, and water passes from the phloem into the xylem through paths like those in a leaf (panel a,iii).

unusual characteristics of transport processes in plants (e.g., flows of liquids at negative pressures in the xylem and against the global gradient in the chemical potential of water in the phloem). For the purposes of this review, we classify these membranes into three categories—physical, osmotic, and active—based on their physicochemical function.

Plasmodesmata: channels formed between the cytoplasm (cell interiors) of adjacent plant cells

Osmosis: the motion of solvent molecules across a semipermeable membrane from a region of low to a region of high solute concentration

Aquaporins: pore proteins in plasma membrane of plant and animal cells that allow for the selective passage of water

We define physical membranes as those that are passive and traversed by pores with diameters too large to provide chemical selectivity (i.e., diameter, $d_p > 1$ nm). In the xylem, physical membranes separate the liquid in the leaves from the atmosphere (**Figure 3a**, panel ii), separate segments of the xylem conduits both laterally and axially along the stem (bordered pit membranes; **Figure 3b**), and separate the sieve tubes of the phloem axially (**Figure 3b**, panel i). In the leaf, these membranes serve as capillary seals that allow for a difference in pressure to exist between the liquid in the xylem and the gas phase outside. In the stem, the bordered pit membranes allow liquid to flow when they are wetted on both sides (**Figure 3b**, panels i and ii), but they serve as capillary seals between a gas-filled segment and an adjacent, liquid-filled segment (**Figure 3b**, panels ii–iv). We can use the Young-Laplace law to provide an estimate of the maximum pressure difference that can be sustained by these capillary seals:

$$\Delta P_{\max} = \frac{4\gamma \cos \theta_r}{d_p}, \quad (1)$$

where γ (Pa m) is the surface tension of water, θ_r is the retreating contact angle on the pore wall, and d_p (m) is the pore diameter (de Gennes et al. 2004). Given that the liquid pressure in the xylem can drop to approximately -10 MPa (**Figure 2**), Equation 1 indicates that the pores in the leaf and bordered pit membranes of these species should have diameters $d_p < 22$ nm [for $\gamma = 7.3 \times 10^{-2}$ (Pa m) and $\theta_r = 0$]. Throughout the xylem path, the membranes are formed of the components of the cell wall (outside the cell's lipid membrane). These components include rigid fibers of cellulose and hydrogels such as pectin (Taiz & Zeiger 2010). The hydrogel component of these membranes could play an important role in defining stabilizing water in the pores of this material (Wheeler & Stroock 2008).

The living cells that form the sieve tubes are connected to one another through pores in their plasma membranes and cell walls at structures called sieve plates; these pores have diameters ranging from 1 to 10 μm (Knoblauch & Oparka 2012) (**Figure 3b**, panel i). The role of these physical membranes in transport through the phloem has remained obscure. They appear to clog with aggregates of proteins, and this process may help in the defense against phloem-feeding insects and limit bleeding from cut tissues. In the leaf, where sugars are loaded into the phloem, the sieve tubes are also connected to some of the source cells by similar pores called plasmodesmata (**Figure 3a**, panel iii). Plasmodesmata act as physical membranes with respect to small molecules but may have small-enough lumens to exclude the passage of macromolecules such as proteins (Turgeon 2010b) (see Section 4.1).

We define osmotic membranes as those that pass solvent (water) but inhibit the passage of small molecules such as sucrose and common ions. In the phloem, osmotic membranes separate the concentrated solutions in the sieve tubes from the nearly pure water in the xylem and the extracellular space (**Figure 3a**, panel iii). This separation allows for an osmotic pressure to be established in living cells; this pressure maintains the turgor of these cells and drives flow in the phloem (Section 3). In the root (**Figure 3c**), these membranes allow for a process of reverse osmosis between the xylem and the water phase in the soil (see Section 3.2.2). The osmotic membranes in plants are formed when the lipid bilayer membrane of a living cell is traversed by water-specific, pore proteins; such proteins are aptly called aquaporins (Taiz & Zeiger 2010).

Active membranes are those that can use biochemical energy to drive the passage of specific species across the membrane. Such membranes have been identified in the loading zone of the phloem in the leaf (**Figure 3a**, panel iii). These membranes are formed where pump proteins traverse the plasma membrane of living cells. The most-studied mechanism involves proton-translocating membrane ATPase, an enzyme that hydrolyzes ATP to drive a flux of protons across

the membrane; the proton gradient then drives the passage of sugars and other solutes across the membrane (Giaquinta 1983).

3. GLOBAL TRANSPORT PROCESSES IN THE XYLEM AND PHLOEM

Theories of the global transport of water and nutrients in plants date back to the end of the 1800s for the xylem [the cohesion-tension (CT) theory] (Boehm 1893, Askenasy 1895, Dixon & Joly 1895) and the middle of the 1900s for the phloem (the Münch hypothesis) (Münch 1930, Horwitz 1958). The English translation of *Palladin's Plant Physiology* has an account of the development of the CT theory (Palladin & Livingston 1926). Despite many alternative proposals (Canny 1995a, Milburn 1996, Zimmermann et al. 2002, Gouin 2008), the basic outlines of the CT theory and the Münch hypothesis remain the most consistent with available experimental data. In this section, we provide a unified but schematic description of these theories (**Figure 4**). We refer readers to Pickard's work for more complete treatments of transport in the xylem (Pickard 1981) and to Jensen et al.'s (2012) recent work on phloem. In Sections 4–6, we provide a more detailed look at particular transport processes that are the focus of current research.

3.1. Water Potential

The presence of multiple phases—vapor, nearly pure liquid, and concentrated solutions—and transfer steps mediated by membranes obliges one to track the driving forces for flows in plants in terms of gradients in the chemical potential of water. Plant scientists express the chemical potential of water in units of pressure and refer to it as the water potential, Ψ_w (Pa):

$$\Psi_w \equiv \frac{\mu_w - \mu_0}{v_l}, \quad (2)$$

where μ_w (J mol^{-1}) is the chemical potential of water, μ_0 is the chemical potential of pure liquid water at atmospheric pressure [P_0 (Pa)], and $v_l = 18.05 \times 10^{-3}$ ($\text{m}^3 \text{mol}^{-1}$) is the molar volume of the liquid phase. Physically, Ψ_w represents the hydrostatic pressure relative to atmospheric pressure in pure liquid water at equilibrium with the phase of interest. We adopt the term water potential in this review to provide a bridge to the literature on plant physiology and because it provides a convenient manner in which to evaluate the impact that a given thermodynamic state of water (e.g., in tissue, the soil, and the atmosphere) will have on transport processes within a plant.

Within a plant and its immediate environment, we can identify important contributions to the water potential (Nobel 1999):

$$\text{liquid: } \Psi_{w,l} = (P - P_0) - RT C_s + \rho_l g z + \Psi_{\text{matrix}} \quad (3a)$$

and

$$\text{vapor: } \Psi_{w,v} = \frac{RT}{v_l} \ln \left(\frac{p_v}{p_{\text{sat}}} \right) + \rho_l g z, \quad (3b)$$

where C_s (mol m^{-3}) is the concentration of solutes, R ($\text{J mol}^{-1} \text{K}^{-1}$) is the ideal gas constant, T (K) is the temperature, $\rho_l = 18.3 \times 10^3$ (kg m^{-3}) is the liquid density, g (m s^{-2}) is the gravitational acceleration, z (m) is the height relative to ground level, Ψ_{matrix} results from interactions of water with a matrix such as tissue or soil, and p_v and p_{sat} (Pa) are the partial and saturation partial pressures in the vapor. The matrix contribution, Ψ_{matrix} , can represent a diversity of interactions that are typically stabilizing (i.e., $\Psi_{\text{matrix}} < 0$), for example, capillary interactions within wettable pores, molecular interactions with a swellable organic material, and interactions of an adsorbate on the surfaces of insoluble materials. The second term in Equation 3a is the osmotic pressure (in the common

Water potential: the Gibb's free energy per unit volume of a phase of water relative to that of pure liquid water at 1 atm

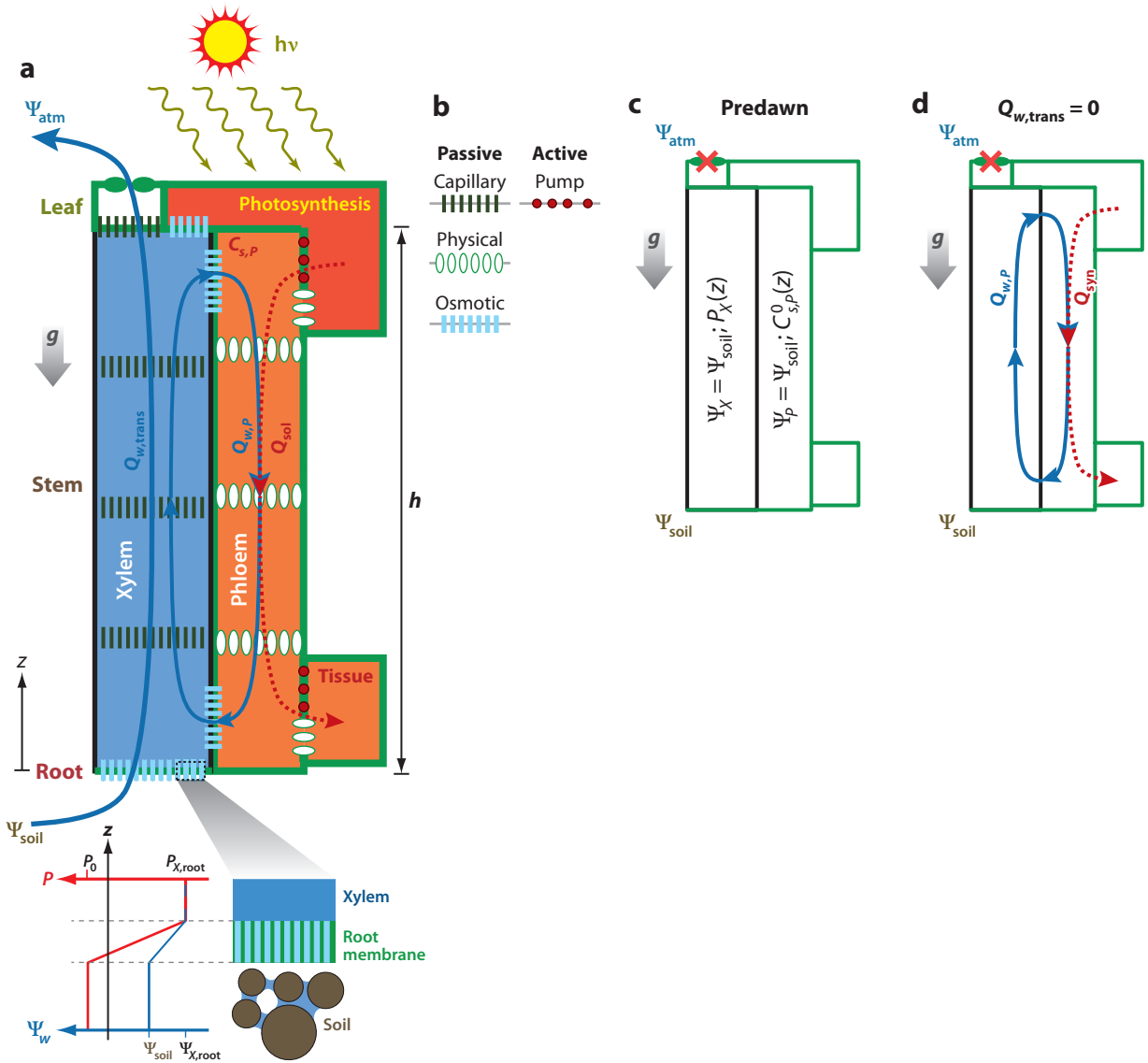


Figure 4

Transport in the xylem and phloem according to the cohesion-tension theory and Münch hypothesis. (a) Simplified, global view with the flows of water associated with transpiration, $Q_w, trans$, and phloem transport, Q_w, p . These flows arise from the difference in the water potential between the soil (Ψ_{soil}) and the atmosphere (Ψ_{atm}) and the flow of solutes loaded into the phloem (Q_{sol}). (Inset) Expanded view of the soil, root membrane, and water in the xylem within a root. Schematic plots show the variations of the pressure and water potential across the root membrane. (b) Identity of the membranes represented in panel a (see Figure 3). (c) Predawn scenario in which the water potential throughout the plant tends toward that of the soil. (d) Nighttime loading of solutes into the phloem, illustrating the Münch pumping mechanism.

approximation for low concentrations, $C_s \ll v_l^{-1}$). The first term of Equation 3b can be thought of as the osmotic pressure of a vapor phase; it too makes a negative contribution to the potential given that typically the relative humidity $p_v/p_{\text{sat}} \leq 1$ such that $\ln(p_v/p_{\text{sat}}) \leq 0$. For a bulk volume of pure liquid at atmospheric pressure and a saturated vapor, one finds that $\Psi_{w,1} = \Psi_{w,v} = 0$.

3.2. Coupled Transport in the Xylem and Phloem

The global demands for mass transfer in plants—the delivery of water and trace nutrients from the soil to leaves and of photosynthetic products (sugars) from the leaves to other tissues—require bidirectional convection between roots and leaves. **Figure 4a** presents a schematic representation of this flow pattern during active transpiration and photosynthesis via the xylem, phloem, and the membranes that couple them to each other, the environment, and other tissues. We use this representation to illustrate the CT and Münch theories in the derivation of steady-state pressures and flow rates as a function of water potentials in the soil (Ψ_{soil}) and the atmosphere (Ψ_{atm}) and the rate at which solutes are loaded into the sieve tubes [Q_{sol} (mol s⁻¹)].

3.2.1. Predawn water potential. To gain an appreciation for the interactions among the various components of the plant and its environment, we first consider the static situation that occurs in the absence of light, as during the night. We take $Q_{\text{sol}} = 0$, although it is known that the leaves can continue to load sugars at night from reserves stored during the day (Hart & Kortschak 1967). Without the potential to photosynthesize or the associated demand for atmospheric CO₂, the stomata remain closed (**Figure 4c**). In this situation, the resistance to the transfer from the leaves to the atmosphere, $R_{X,\text{leaf}}$ (mol s⁻¹ Pa⁻¹), diverges, the net flow of water from the soil to the atmosphere is minimal, and all the coupled compartments filled with water approach equilibrium with that in the soil: $\Psi_X = \Psi_P = \Psi_{\text{soil}}$. In this situation, we can solve Equation 3a for the pressure within the nearly pure liquid ($C_{s,X} \cong 0$) within the xylem:

$$P_X(z) = P_0 - \rho_l g z + \Psi_{\text{soil}}. \quad (4)$$

We take $\Psi_{X,\text{matrix}} = 0$ because water exists as a bulk liquid phase in the xylem without significant interactions with the tissue. In the portion of the xylem above ground, gravity lowers the pressure, and for $z > 10$ m, it drops below zero (negative pressure or tension). For pressures below that at coexistence [the saturation vapor pressure, $p_{\text{sat}}(T)$], the liquid is superheated and metastable with respect to boiling; for negative pressures, the liquid can be considered to be in a stretched, superheated state (DeBenedetti 1996, Wheeler & Stroock 2009). This metastability represents a liability to plants: The liquid in the xylem is prone to boiling (also referred to as cavitation or embolization) and an associated loss of conductance. We return to this liability in Section 3.3.

More often than not, $\Psi_{\text{soil}} = \Psi_{\text{soil,matrix}}$ is negative and can act as the dominant origin of the reduced pressure within the xylem such that tension can exist even at the base of plants and in plants of modest stature (<10 m) when the soil is subsaturated. The data of Scholander et al. (1965) illustrate this phenomenon (**Figure 2**). First, the nighttime pressure in mangroves (*Rhizophora*), with their roots submerged in brine, is approximately -30 bars (-0.3 MPa); this corresponds closely to the osmotic pressure of seawater. Second, arid climate shrubs have significantly larger tensions in their xylem than much taller species such as redwoods in humid climates. Plant scientists exploit the equilibrium expressed in Equation 4 to measure the water potential in the soil: Before the sun rises, they will take a reading of the pressure in the xylem (typically with a Scholander pressure chamber). They take the predawn value of Ψ_X as an estimate of Ψ_{soil} .

In contrast with the case of the xylem, plants actively manage the thermodynamic state of water in the phloem such that its pressure remains greater than atmospheric pressure. To maintain this

Transpiration: the flow of water from the soil to the leaf of a plant due to the thermodynamic gradient of water potential between the air and leaf water

Metastable liquid: a liquid phase that is kinetically stable but thermodynamically unstable with respect to its vapor phase (superheated) or its solid phase (supercooled)

positive relative pressure or turgor pressure ($\Delta P_{\text{turgor}} = P_p - P_0 > 0$), metabolically active cells adjacent to the phloem secrete solutes (principally sugars) into the sieve tube. This persistent overpressure in the phloem may be necessary to avoid the collapse of the sieve tubes (Smith & Milburn 1980) and to expel phloem-feeding insects (Turgeon 2010a). Osmotic membranes that exclude passage of these solutes couple the phloem to the xylem and also to the soil (**Figures 3a,c** and **4a,b**). At equilibrium with the soil ($\Psi_p = \Psi_{\text{soil}}$), we can solve Equation 3a for the concentration of solutes within the phloem:

$$C_{s,p}^0(z) = \frac{1}{RT} (\Delta P_{\text{turgor}} + \rho_l g z - \Psi_{\text{soil}}) \quad (\text{mol m}^{-3}), \quad (5)$$

where we assume $\Psi_{p,\text{matrix}} = 0$ because the aqueous solution exists as a bulk phase in the phloem. Equation 5 provides an example of a general strategy by which plants use changes in the distribution of solutes (with expenditure of biological energy) to manipulate the stress within their cells and conduits for structural stability, growth, and motion (Taiz & Zeiger 2010).

3.2.2. Net transport during photosynthesis: transpiration. In the common scenario in which the atmosphere is drier than the soil ($\Psi_{\text{atm}} = \Psi_{\text{soil}} - \Delta \Psi_{s-a} < \Psi_{\text{soil}}$), the flow of water from the roots to the leaves occurs spontaneously along this external gradient in the water potential. Critically, the coupling via membranes in the roots and leaves converts the difference in Ψ_w between distinct phases [e.g., matrix bound water in the soil, $\Psi_{\text{soil}} = \Psi_{\text{matrix}} \leq 0$, and subsaturated vapor in the atmosphere, $\Psi_{\text{atm}} = (RT/v) \ln(p_v/p_{\text{sat}}) + \rho_l g z \leq 0$] into a difference in pressure within the liquid in the xylem. This conversion allows the plant to offer a path of high conductance for water out of the soil and up to the leaves. We note that the process of transpiration from a subsaturated soil ($\Psi_{\text{soil}} < 0$) is a remarkable variant of purification by reverse osmosis (the expanded view of transport across the root membrane in **Figure 4a**): Water exits the leaf by evaporation into subsaturated air ($\Psi_{\text{atm}} < \Psi_{X,\text{leaf}} < \Psi_{X,\text{root}} < \Psi_{\text{soil}}$) such that the pressure in the xylem drops, typically into tension. Information about the reduced water potential in the atmosphere is transmitted as tension to the root through the column of pure liquid in the xylem. This tension pulls water out of the root membrane until it reaches a water potential below that of the soil. Pure liquid water then partitions into the root membrane from the subsaturated phase in the soil. Unlike conventional reverse osmosis (Probstein 1994), tension in the purified phase (within the xylem) drives the process rather than elevated pressure in the subsaturated phase. In this sense, plants perform reverse reverse osmosis. In an alternative perspective, transpiration can be seen as membrane distillation at a distance (McCabe et al. 2005).

3.2.3. Net transport during photosynthesis: phloem transport. The photosynthesis of sugars in the leaf provides an elegant mechanism with which to generate a pressure-driven flow in the sieve tubes, running counter to the flow in the xylem and counter to the global gradient in the water potential. We use the simplified, steady-state scenario depicted in **Figure 4a** to illustrate this mechanism originally proposed by Münch (1930). As these sugars are loaded into the phloem in the leaf, the concentration of the solutes will rise [above its static value, $C_{p,s}^0(z)$; Equation 5] until the water potential drops below that in the adjacent xylem vessels: $\Psi_{p,\text{leaf}} < \Psi_{X,\text{leaf}}$. Water will pass through the osmotic membrane separating the phloem from the xylem in response to this gradient such that the local pressure rises and flow down the sieve tube begins. This convection in the phloem delivers the sugars to the tissue within the stem and root. At steady state, the rate of solute loading, Q_{sol} (mol s^{-1}), must balance the rate of depletion such that the concentration at the base of the plant returns to its static value (Equation 5). If we assume that the tissues surrounding

the sieve tubes and other sinks (e.g., fruits) do not deplete water from this flow, then it must pass back into the xylem and up the plant. The synthesis and loading of sugars thus provide a second driving force for the circulation of fluids within plants.

3.2.4. Analysis of coupled flows in the xylem and phloem. We can use the scenario depicted in **Figure 4a** to derive simple relationships among the driving forces, $\Delta\Psi_{s-a} = \Psi_{\text{soil}} - \Psi_{\text{atm}}$, and rate of solute loading, Q_{sol} ; the flows related to transpiration, $Q_{w,\text{trans}}$ (mol s^{-1}) and phloem transport, $Q_{w,p}$ (mol s^{-1}); and the additional concentration of solutes in the phloem, $\Delta C_{p,s}$ (mol m^{-3}) relative to the static value. We note that this treatment is just one of many models that can be proposed for coupled flow in the phloem and xylem. Currently, too little is known about either the physiology or the dynamics of the phloem to fully constrain transport models with respect to boundary conditions, conductances, and modes of biological regulation (Knoblauch & Oparka 2012). The generalized momentum balances can be expressed as follows for a plant of height h (**Figure 4**):

$$\Delta\Psi_{s-a} = \Psi_{\text{soil}} - \Psi_{\text{atm}} = \Delta P_X + Q_{w,\text{trans}}(R_{X,r} + R_{X,l}) - \rho_l g h, \quad (6a)$$

$$\Delta P_X = P_{X,r} - P_{X,l} = R_X(Q_{w,\text{trans}} - Q_{w,p}) + \rho_l g h, \quad (6b)$$

$$\Delta P_P = P_{P,l} - P_{P,r} = R_P Q_{w,p} - \rho_l g h, \quad (6c)$$

and

$$RT\Delta C_{s,p} = (2R_{X-p} + R_P)Q_{w,p} + \Delta P_X - \rho_l g h = R_{P,\text{tot}}Q_{w,p} + \Delta P_X - \rho_l g h. \quad (6d)$$

The resistances from the soil into the root, $R_{X,r}$ ($\text{Pa}\cdot\text{s mol}^{-1}$), and the leaf into the atmosphere, $R_{X,l}$, include those to mass transfer due to the membranes and due to the transfer from the external phase to the membrane; for the leaf, $R_{X,l}$ also includes the resistance associated with the stomata (**Figure 3a**, panel i), the value of which is actively controlled by the plant. The resistance R_{X-p} ($\text{Pa}\cdot\text{s mol}^{-1}$) is that of the osmotic membranes separating the xylem and phloem (assumed to be equal in the leaf and root). The resistances R_X and R_P ($\text{Pa}\cdot\text{s mol}^{-1}$) are associated with Poiseuille flow through the xylem capillaries and phloem sieve tubes, respectively (these resistances are often dominated by passages through end walls and sieve plates). We need one additional relationship to couple the osmotic pressure ($RT\Delta C_{p,s}$) to the flows. If we assume that the evacuation of solutes at the bottom of the phloem is fast, a steady-state species balance in the sieve tube between production (Q_{sol}) and convective mass transfer with the phloem flow ($Q_{w,p}$) gives

$$\Delta C_{s,p} = \frac{\text{production (mol s}^{-1}\text{)}}{\text{volumetric flow (m}^3 \text{s}^{-1}\text{)}} = \frac{Q_{\text{sol}}}{v_l Q_{w,p}}. \quad (7)$$

Uniting Equations 6 and 7, we find the following relations for the phloem and transpiration flows:

$$a Q_{w,p}^2 + b Q_{w,p} + c = 0 \text{ with} \\ a = \frac{R_{P,\text{tot}}}{R_X} + \frac{R_{X,r} + R_{X,l}}{R_{X,\text{tot}}}, \quad b = \frac{\Delta\Psi_{s-a}}{R_{X,\text{tot}}}, \quad \text{and } c = -\frac{Q_{\text{sol}}}{R_X} \frac{RT}{v_l}, \quad (8)$$

and

$$Q_{w,\text{trans}} = \frac{\Delta\Psi_{s-a} - R_X Q_{w,p}}{R_{X,\text{tot}}}, \quad (9)$$

where $R_{X,\text{tot}} = R_{X,r} + R_X + R_{X,l}$. The quadratic form for $Q_{w,p}$ arises from the coupling in Equation 6 between the synthesis and flow.

We consider nighttime loading of solutes to illustrate how the coupling of the xylem and phloem allows the synthesis of sugars to drive downward flow in the phloem. At night, we take the stomata to be closed ($R_{X,l} \rightarrow \infty$) and allow for continued loading of sugars ($Q_{\text{sol}} > 0$) (**Figure 4d**). In this limit, Equations 7 and 8 give

$$Q_{w,p} = \left(\frac{RT/v_l}{R_{p,\text{tot}} + R_X} Q_{\text{sol}} \right)^{1/2} \quad \text{and} \quad \Delta C_{s,p} = \left(\frac{R_{p,\text{tot}} + R_X}{v_l RT} Q_{\text{sol}} \right)^{1/2}. \quad (10)$$

Here, with complete decoupling from the global gradient in the water potential, the synthesis and loading of sugars drive the flow of solutes down the phloem. This osmotic pump requires that pure water is brought into the leaves by the xylem; if the phloem were the only conductive path, then there would be no means of driving steady-state flow by this mechanism. The scaling $Q_{w,p} \sim Q_{\text{sol}}^{1/2}$ arises from the dependence of the concentration on the rate of convection (Equation 6). A consequence of this scaling is that the flow rate and associated pressure in the phloem vary more slowly with the height of the plant (via the resistances $R_{p,\text{tot}}$ and $R_X \sim \text{height}$, $Q_{w,p} \sim \text{height}^{-1/2}$) than they would for a mechanical pressure pump ($Q \sim \text{height}$ for constant driving force). A weak dependence of phloem pressures on height has been noted across species (Turgeon 2010a). In the general case with active transpiration (stomata open) and sugar loading (**Figure 4a**), this osmotic pump runs in parallel with the evaporation-driven transpiration. We see how the strategic use of membranes and the generation of an opposing gradient in the chemical potential of solutes (experienced by water as a gradient in osmotic pressure) allow plants to satisfy their need for bidirectional flows.

The general solutions of Equations 8 and 9 predict coupling between the two flows: The transpiration rate will be a function of the rate of sugar loading, and the phloem flow will be a function of $\Delta\Psi_{s-a}$. Experiments testing this coupling have not been reported, hindered, in particular, by a lack of access to rates of loading and flow in the phloem. We finish this subsection by noting that gravity only affects the flow rates in the xylem and phloem (Equations 8 and 9) through the water potential of the atmosphere (Equation 3b). For example, taller plants will transpire more slowly than shorter ones at a given relative humidity. The impact of gravity also appears in the static gradient in the pressure in the xylem (Equation 4) and in the concentration of the solute in the phloem (Equation 5).

3.3. Further Considerations of the Cohesion-Tension and Münch Mechanisms

Although plant scientists generally agree with the global features of the CT and Münch mechanisms as described in Sections 3.1 and 3.2, there are ongoing efforts to achieve complete experimental validation of their predictions and to define the details of specific physiological components (e.g., physicochemical and biological properties of the membranes). In this subsection, we provide an overview of some consequences of these theories, relevant experiments, and outstanding questions. In Sections 4–6, we pursue some of these topics further.

3.3.1. The tension in cohesion-tension theory. As stated in Section 3.2.1, the water in the xylem often exists at pressures below atmospheric pressure such that the column of liquid is prone to breakage by the formation of bubbles. For mildly reduced pressures in the range $p_{\text{sat}} \leq P_X < P_0$, the liquid, which has been in contact with air at 1 atm, becomes supersaturated with dissolved gases and thermodynamically unstable with respect to the formation of air bubbles. For larger reductions of pressure ($P_X < p_{\text{sat}}$), the liquid also becomes thermodynamically unstable with respect to the formation of vapor bubbles or boiling. This doubly unstable situation sounds disastrous, but it

need not be because both these thermodynamically unstable states (supersaturation and superheat) can be kinetically stable (metastable) owing to the activation energy associated with the formation of a gas nucleus in the liquid (DeBenedetti 1996). Furthermore, nucleation theories (appropriate for both supersaturation and superheat) predict that this kinetic stability should persist down to pressures below -100 MPa in the absence of pre-existing nuclei (Herbert & Caupin 2005). Experiments based on isochoric cooling of liquid water agree reasonably well with the predicted stability limit (Zheng et al. 1991, Azouzi et al. 2013). Pressures below -20 MPa are reached in experiments in a synthetic system that mimics the CT mechanism of coupling the liquid to a subsaturated phase via a capillary membrane that mimics the leaf membrane (**Figure 3a**; Equation 3) (Wheeler & Stroock 2008). From the data in **Figure 2** (Scholander et al. 1965), we conclude that plants do not operate anywhere near either the fundamental stability limit of water or the practical limit of the CT mechanism. In Section 5, we discuss the observed stability limit in plants, the possible origins of this limit, and mechanisms of recovery.

3.3.2. Loading and unloading the phloem. Although the Münch mechanism implicates more familiar physical regimes and processes than CT theory does, it involves the complex physiology of living tissues, which has proven difficult to access experimentally. For example, questions remain with respect to the size, number, and distribution of loading and unloading zones for solutes into and out of the phloem sieve tubes (Thompson 2006, Knoblauch & Peters 2010). More basic challenges for the Münch mechanism also persist. In particular, as noted in Section 3.2.4, osmotic pressures measured in sieve tubes do not scale with the height of a plant as one would expect (Turgeon 2010a). This effect may result from species-to-species differences in the distribution of loading and unloading zones or from differences in the resistance of the sieve tubes or may point to a more basic flaw in the theory. In Section 6.2, we discuss one successful use of the Münch theory to the scaling of morphological properties across a broad set of data on trees.

4. CONTROL OF FLOW

The CT and Münch mechanisms (Section 3) elucidate the global driving forces of flow— $\Delta\Psi_{s-a}$ for transpiration and Q_{sol} for phloem flow—but they do not specify the points of control. Plants must manage both global and local fluxes of water and solutes to maintain hydration, direct signaling molecules, and distribute resources. We can gain insights into the logistics and mechanisms of some of these control strategies with physicochemical arguments.

4.1. Global Control

Plants cannot control $\Delta\Psi_{s-a}$, so which resistance along the path provides the most-sensible point of control for the global rate of transpiration? Physical considerations point to the resistance of the stomata that sit in the path of vapor diffusion between the interior surfaces of the leaf and the atmosphere: As discussed in Section 3.2.1, closure of the stomata (increasing $R_{X,t}$) allows the liquid water within the xylem to approach the water potential in the soil, the highest in the system. This strategy minimizes the degree of metastability in the liquid and thus its fragility with respect to cavitation. Restricting flow anywhere upstream of the leaf (lower on the plant, e.g., at the root or along the stem) would force the downstream fraction of the liquid to approach the water potential of the atmosphere, the lowest in the system. From a biological perspective, this solution is a compromise because restricting the conductance of the stomata also limits the uptake of CO_2 and thus the rate of photosynthesis. To moderate this compromise, plants control stomatal conductance with both positive feedforward from the photosynthetic rate and negative feedback

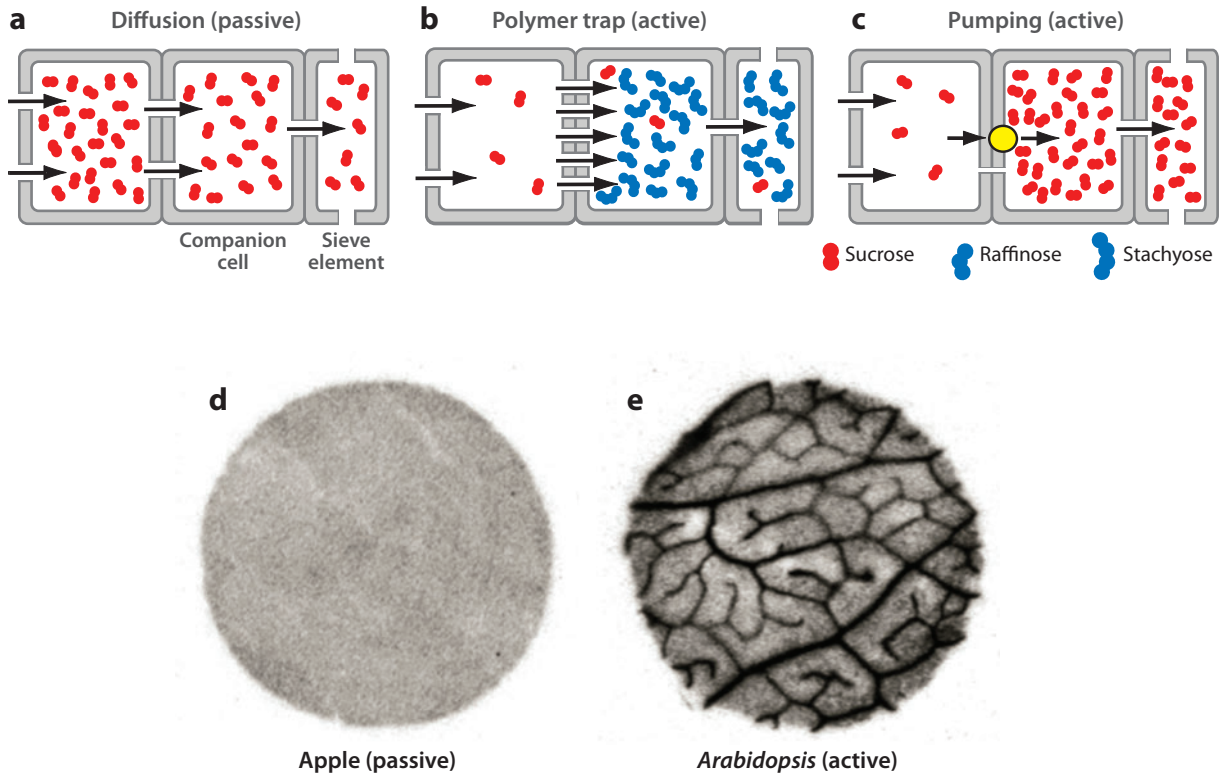


Figure 5

Mechanisms of phloem loading. (a) Passive loading based on diffusion in a companion cell and sieve element, a component of the sieve tube. (b) Active loading by the polymer trap mechanism. Enzymes in companion cells and sieve elements polymerize sucrose into raffinose and stachyose. (c) Active loading based on protein pumps (yellow circle). (d,e) Autoradiographs of leaves incubated with isotope-labeled sucrose. Active loading leads to visible concentrations of sucrose in phloem vessels (e). Figure adapted with permission from Turgeon (2010b).

from the water potential in the leaf. Analyses of this coupled dynamics originating with models proposed by Cowan (1972) are consistent with experimental observations, including the curious but common phenomenon of spontaneous, temporal oscillations in stomatal opening (Farquhar & Cowan 1974). Rand (1983) has analyzed the mechanics and dynamics of stomatal control, as reviewed previously.

Given that flow in the phloem serves to export solutes, one obvious point of flow control is in the loading zone for solutes within the leaf. At least three distinct mechanisms have been observed for the loading of sugars into the phloem (Turgeon 2010b) (Figure 5). First, the simplest is by passive molecular diffusion through a series of physical membranes from the photosynthetic cells to the sieve tubes (Figure 5a). This mechanism requires higher concentrations of sugars in leaf cells (companion cells) than in sieve elements. Second, an active mechanism called polymer trapping has been elucidated recently. Sucrose (a disaccharide) diffuses through plasmodesmata into companion cells and sieve elements, where oligomerization into larger sugars (tri- and tetrasaccharides) occurs enzymatically with the expenditure of metabolic energy (Figure 5b) (Turgeon 2010b). The current understanding indicates that the flux of sugars is rectified because the oligomers are too large to pass back to the source cells. Third, another active mechanism involves the pumping of solutes

by transporter proteins that traverse the plasma membranes (lipid bilayer) that separate some companion cells from the sieve tubes (**Figure 5c**) (Giaquinta 1983). For a given concentration of sugars in the source cells, the active mechanisms allow for the buildup of higher concentrations of sugars than the passive transfer does. **Figure 5d,e** shows the difference in the distribution of sugars in passive and active loading species, respectively. The higher osmotic pressure associated with active loading could aid in the transfer of solutes over long distances. Interestingly, however, many of the tallest species in the world (e.g., conifers such as redwoods) appear to lack active loading mechanisms (Fu et al. 2011). Turgeon (2010b) recently used a full plant growth model to suggest that the selective advantage of active loading may relate its ability to rapidly export a larger fraction of the newly synthesized sugars to growing tissues rather than storing them in the leaf to drive passive diffusion. He pointed to the importance of this efficiency in rapidly growing herbaceous (leafy perennials) plants. Although it is significantly less well characterized, unloading may also serve as an important point of control of phloem flows (Goeschl et al. 1976, Thompson & Holbrook 2003).

4.2. Local Control

The possibility that plants have strategies to control flows locally within the xylem has emerged in the past few decades. The control of conductance at the level of individual xylem vessels within the stem could allow plants to redistribute flow, for example, to compensate for the spatial heterogeneity of the water potential in the soil or evaporative demand in the atmosphere. This possibility challenges the conventional picture of the xylem as inert deadwood. The idea arose from a curious observation reported by Zimmermann (1978): The hydraulic conductance of excised stem segments was up to 50% higher when perfused with tap water than with distilled water. Subsequent studies reproduced this result in a variety of species and identified changes in ionic strength and pH as the most important effectors of changes in conductance. In most studies, higher ionic strength leads to higher conductance, and higher pH leads to lower conductance (van Ieperen et al. 2000, Zwieniecki et al. 2001, López-Portillo et al. 2005, Domec et al. 2007, Nardini et al. 2007). Further experiments by Zwieniecki et al. (2001) suggested that the membranes in the bordered pits dominate this response.

Figure 6 illustrates a typical experiment and response to variations in ionic strength in the perfused fluid. Zimmermann (1978) proposed two explanations that have since been developed further. First, poly(electrolyte) hydrogels in the flow path respond to changes in ionic strength and pH by changing their degree of hydration via Debye screening of charged sites and the protonation/deprotonation of acid moieties. Pectin poly(saccharides) are found in many plant tissues and form hydrogels with pH-sensitive charge. Using atomic force microscopy on the surface of bordered pit membranes of tobacco plants, Lee et al. (2012) observed changes in surface morphology with changes in ionic strength that are consistent with the presence of hydrogels. No one has presented a formal model of the coupling of gel swelling to transport. Second, electrokinetic phenomena couple the state of bond charges within the membranes to the flow (Probstein 1994). The pressure-driven flow convects the mobile net charge in the screening layer and establishes a streaming potential; this potential drives an electroosmotic flow that counters the pressure-driven flow. This electroviscous effect is well established in synthetic systems (Bowen & Jenner 1995), and streaming potentials have been observed in the xylem (Tyree & Zimmermann 1971). Van Doorn et al. (2011) presented a simple model of this effect that agrees qualitatively with many observations (increasing conductance with increasing ionic strength across the physiological range). Further experiments are necessary to distinguish between these proposals and to establish how plants might actively modulate the local ionic strength to exploit this means of regulating flow.

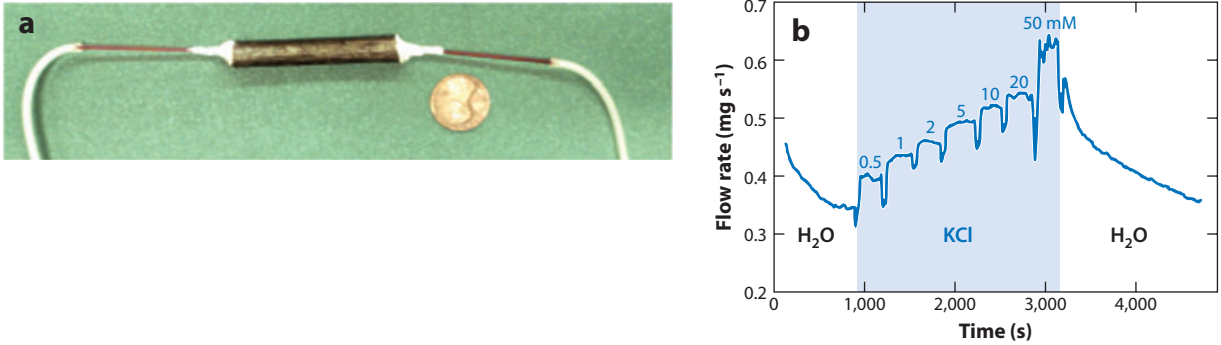


Figure 6

Variable conductance of the xylem as a function of the composition of sap. (a) The perfusion of an individual xylem vessel in an excised section of stem. (b) Measured flow rate at a constant pressure drop through a section of the xylem as in panel a. The composition of the liquid perfusate was changed from deionized water to a series of solutions of potassium chloride and back to deionized water. Figure adapted with permission from Zwieniecki et al. (2001).

5. EMBOLIZATION AND RECOVERY

In Section 3.3.1, we point out that plants do not seem to approach the ultimate tensile strength of liquid water during transpiration. Nonetheless, the breakage of the liquid columns in the xylem does occur, with important consequences for plant function and viability.

5.1. The Stability Limit in Plants

Multiple types of measurements provide evidence for the cavitation of the liquid in the xylem. Most directly, the emptying of individual segments can sometimes be observed optically in narrow stems or via cryosectioning and imaging by electron microscopy (Marenco et al. 2006). Less directly, in woody species, one can detect cavitation events in the xylem acoustically, in real time with an ultrasonic transducer pressed against the external surface of a stem or trunk. The rapid growth of a gas bubble within a vessel segment can emit an ultrasonic click with frequencies in the range 0.1–1 MHz via the release of elastic energy in the woody tissue (Milburn & Johnson 1966, Tyree & Dixon 1983). The emission of sounds by events other than cavitation (e.g., the withdrawal and imbibition of water from nonconductive tissues and the solid mechanical failure of woody elements) complicates the interpretation of acoustic signals (Tyree & Dixon 1983). A functional assay of cavitation involves excising a section of stem from a plant at a known water potential and measuring its hydraulic conductance (e.g., as in **Figure 6a**) immediately after excision and after full rehydration (Tyree & Sperry 1989). The relative conductance or percent loss of conductance (PLC)—embolized to rehydrated—provides a measure of the fraction of vessels that were empty at the moment of excision. The PLC rises with decreasing water potential in the xylem.

Figure 7 presents a compilation for 223 species of the typical, minimum water potential observed in the leaf or needle, Ψ_{\min} , as a function of the water potential that leads to a 50% loss of conductivity, Ψ_{50} (Choat et al. 2012). The distance of points above the 1:1 line provides a measure of the margin of safety with respect to a substantial loss of xylem conductance owing to cavitation. These data indicate that many plants (in particular, angiosperms) live at or near their stability limit. Choat et al. (2012) pointed to potential implications of this dangerous lifestyle on the response of plants to climate change. We note, however, that plants can recover from partial

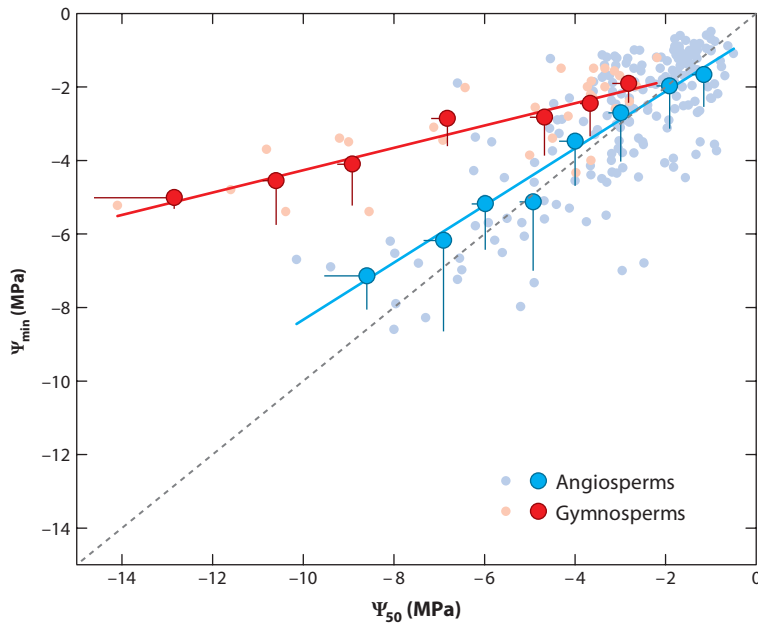


Figure 7

Stress and vulnerability to embolization in 191 angiosperm and 32 gymnosperm species. Ψ_{\min} is the typical daily minimum in the xylem water potential. Ψ_{50} is the water potential corresponding to a 50% loss of conductance. Faint, filled symbols correspond to measurements on an individual species. Dark, filled symbols present averages of the individual data in bins of 1 MPa. The dashed line represents 1:1. Figure adapted with permission from Choat et al. (2012).

embolization (see Section 5.2) and that the lethal threshold for the loss of conductance depends on the species. For example, for the angiosperms that fall below the 1:1 line in **Figure 7**, this lethal PLC must be greater than 50%. This interspecies variability complicates the evaluation of risk implied by this meta-analysis.

The onset of cavitation indicated in **Figure 7** (−1 to −8 MPa) is much lower than the predicted stability limit for homogeneous nucleation (Herbert & Caupin 2005). Although no definitive answer exists for the mechanism of nucleation that sets the stability limit in the xylem, one telling experimental observation is that the magnitude of the limiting pressure (tension) is similar to the pressure required to force air through the wetted bordered pit membranes that separate the vessel segments in the xylem (**Figure 3**) (Cochard et al. 1992). [These experiments are the same as those used in capillary flow porometry to characterize the distribution of pore sizes in a membrane (Lowell & Shields 1991).] This observation suggests that cavitation may occur when air is pulled into a liquid-filled segment of the xylem through membranes that separate it from air-filled pockets in the stem (**Figure 3b**). In other words, the xylem may be designed with safety valves that allow for the seeding of nucleation at a biologically defined pressure. Such a safety threshold may be necessary to avoid damage that could arise during higher-energy cavitation events at lower pressures; the destructive tendencies of cavitation bubbles are well documented in hydrodynamic and ultrasonic cavitation (Philipp & Lauterborn 1998). Of course, as is familiar in the study of superheated liquids and boiling, other heterogeneous mechanisms of bubble nucleation can define a limit of metastability far below that predicted for homogeneous nucleation (Lahey 1992); the role of such heterogeneous processes in plants has not been excluded.

5.2. Recovery from Embolization

As mentioned above, plants can recover from the conductivity loss of the xylem that occurs as a result of embolization. For example, one observes that the loss in conductance that develops during the day can be recovered during the night, presumably based on the refilling of embolized vessels with liquid water (Zwieniecki & Holbrook 1998, Zufferey et al. 2011). Recently, magnetic resonance imaging (Holbrook et al. 2001) and X-ray tomography (Brodersen et al. 2010) have allowed for visualization of refilling *in vivo*. **Figure 8a** shows X-ray tomography images of an intact grapevine (Brodersen et al. 2010). Initially, multiple sections of the vessels in the field of view are filled with air; over a period of 3.8 h, these zones fill with water. **Figure 8b** presents a three-dimensional reconstruction of an intermediate state during refilling. We infer from the apparent segregation of liquid into droplets in **Figure 8b** that the walls of the xylem are not fully wetting; independent optical measurements indicate contact angles of $\sim 40\text{--}50^\circ$ for water on the xylem (Zwieniecki & Holbrook 2000). This partial wetting condition means that capillary spreading cannot aid in the initiation of refilling. Given that the metastability of the liquid in the xylem may persist even in the absence of transpiration (Equation 3), the refilling process poses a physical challenge: To expel the air and vapor from the embolized vessel, the plant must either raise the pressure in adjacent vessels to above P_0 (assuming the air within the vessels has come to equilibrium with the ambient air pressure) to push the liquid back into the vessels or employ another means of reversing the local gradients of the water potential.

Plant scientists have long recognized the ability of some plants to accumulate solutes in the xylem of their roots when transpiration is stopped (via a Münch-like mechanism; see Section 3.2.1) such that water can be recruited from the soil and positive relative pressures can be developed (Slatyer 1967). A survey across species indicated that this root pressure can reach 0.1–0.2 MPa above atmospheric pressure (Fisher et al. 1997) and could thus explain the repair of embolized vessels at night in smaller species with well-hydrated soil (Tyree & Yang 1992, Lewis et al. 1994). Starting in the 1980s, reports of recovery in the presence of active transpiration and negative water potentials (Salleo & Lo Gullo 1989; Canny 1995b, 1997; Salleo et al. 1996; Hacke & Sperry 2003) suggested that alternative mechanisms were required. To date, Brodersen et al.'s (2010) X-ray computed tomography observations represent the only report of the direct observation of refilling under tension (**Figure 8a,b**).

Refilling in the presence of tension in adjacent vessels requires (a) the induction of an energy-dissipating process that locally pumps liquid into the emptied vessels (Canny 1997, Holbrook & Zwieniecki 1999) or lowers the water potential in the vessel (e.g., with the secretion of solutes; **Figure 8c**) such that water is drawn in spontaneously (Salleo et al. 1996, Tyree et al. 1999, Hacke & Sperry 2003, Zwieniecki & Holbrook 2009) and (b) a mechanism by which the liquid in the refilled vessel reconnects with the adjacent columns of liquid under tension (Holbrook & Zwieniecki 1999, Tyree et al. 1999, Zwieniecki & Holbrook 2009). With respect to the first process, multiple investigators have reported evidence for solutes in the xylem after cavitation (Canny 1997; Secchi & Zwieniecki 2010, 2011), a dependence of refilling on the phloem (Salleo et al. 2004, Nardini et al. 2011), and metabolic activity in living tissue adjacent to embolized vessels (Salleo et al. 2009, Secchi & Zwieniecki 2010, Secchi et al. 2011). These studies suggest that plants may use the transfer of solutes to induce local refilling of embolized vessels. The second challenge is purely fluid mechanical in nature (Holbrook & Zwieniecki 1999). Once an embolized vessel has reached a nearly full state (depicted in **Figure 8d** based on the secretion of solutes into the embolized vessel), the refilling solution will still be at positive pressure, in mechanical equilibrium with the remaining air (**Figure 8d**). Once the refilling solution moves into a single pit and contacts the membrane (the upper pit in **Figure 8e**), the hydraulic coupling

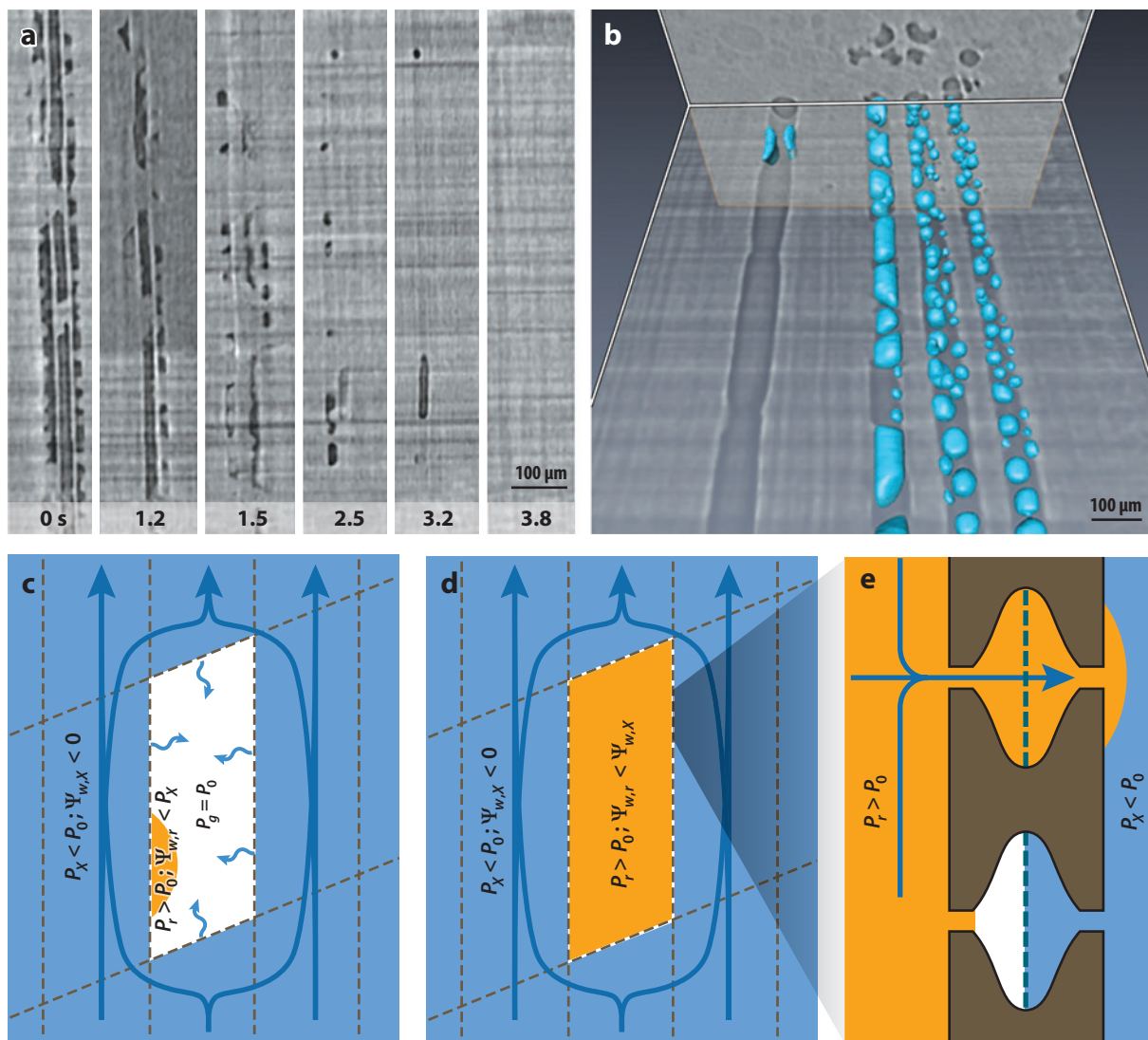


Figure 8

Refilling embolized vessels. (a) X-ray computed tomography images and (b) reconstruction of the xylem in an intact grapevine. In panel a, the six frames show the evolution of a section of the xylem over 3.8 h. Dark areas correspond to gas-filled sections of the vessel. In panel b, a single instant during refilling is shown, with the voxels identified as water rendered in three dimensions and false-colored in blue. (c–e) Schematic depictions of a hypothesis for local refilling with a negative water potential. Solutes secreted into an embolized vessel initiate the growth of a droplet of refilling solution with the water potential, $\Psi_{w,r}$, below that of the liquid in the surrounding vessels in which the liquid remains metastable ($\Psi_{w,X} = P_X - P_0 < 0$) (c). The pressure in the gas goes to atmospheric pressure ($P_g = P_0$), and the pressure in the refilling solution must be greater than atmospheric pressure ($P_r > P_0$). As filling approaches completion (d), the narrow openings of the bordered pits catch the meniscus (depicted in the bottom pit in panel e). Once the refilling solution breaks into a single pit and contacts the membrane (depicted in the upper pit in panel e), the hydraulic coupling to the external liquid at lower pressure will tend to empty the newly filled segment. Panels a and b adapted with permission from Brodersen et al. (2010).

Embolism: gas-filled section of xylem that results from cavitation and obstructs water transport through the xylem

to the external liquid at lower pressure will tend to empty the newly filled segment. It appears the refilling could be a Sisyphean task: The meniscus would need to enter each bordered pit nearly simultaneously, or the first contact with the external fluid would reset the process. One proposal for resolving this apparent paradox suggests that the variable shape and wetting properties of the bordered pits pin the advancing meniscus (the bottom pit in **Figure 8e**) such that it arrives at the bordered pit membranes in a nearly synchronized manner (Holbrook & Zwieniecki 1999, Konrad & Roth-Nebelsick 2003).

6. TRANSPORT-RELATED CONSTRAINTS ON PLANT MORPHOLOGY

6.1. Maximum Tree Height

As indicated in Equations 3 and 4, the gravitational pressure head places mechanical and thermodynamic constraints on liquids in the xylem and phloem: At increasing height within a plant, both the metastability (superheat) in the xylem and the required concentration of solute in the phloem rise. Presumably, accommodating these constraints results in costs for the plant as it grows taller. For example, increasing tension may require thicker walls for the xylem conduits and more elaborate mechanisms to withstand and recover from increasingly probable cavitation events. Maintaining turgor at lower water potentials may force the plant to store sugars in the leaf that could otherwise have served in other tissues. Recent studies have reported monotonic trends in some physiological properties (vessel and membrane structure, embolism threshold, photosynthetic efficiency, turgor pressure) as a function of height; these trends suggest adaptation to costs related to height (Woodruff et al. 2004, Domec et al. 2008, Ambrose et al. 2010). By extrapolating these empirical trends to the height at which loss of viability would be expected (e.g., owing to the complete loss of conductivity), these studies have suggested that the maximum heights of specific species may be set by constraints on the xylem and phloem. Such arguments depend on a large number of assumptions because of the complexity of interconnected evolutionary (Sperry 2003), ecological (Cramer 2012), and growth (Ryan & Yoder 1997, Netting 2009) phenomena that together determine observed traits; they should be treated with caution. Not surprisingly, to date, no complete argument exists to explain the observed maximum heights of plants.

6.2. Allometry

Attempting to explain scaling relationships between physiological structures represents a more tractable, yet still challenging goal. Many such allometric relationships have been identified for plants (Niklas 1994). In pursuing explanations for relationships between internal components of individual plants, rather than the magnitude of a specific property, one has the potential to isolate rules defined by constraints intrinsic to the organism (e.g., material properties, fundamental laws of geometry and conservation) and less influenced by extrinsic constraints related to the environment and ecology (LaBarbera 1990). Murray's law for the variations in the diameter of blood vessels in mammals provides a successful example of such an analysis. Based on a minimization of metabolic power for the maintenance of blood and blood flow, Murray (1926) predicted that at each branch point in a vascular network, the sum of the cubes of diameters of daughter vessels equals the cube of the diameter of the parent vessel (LaBarbera 1990). Interestingly, McCulloh et al. (2004) reported the applicability of Murray's law to the architecture of the xylem in specific tissues and species in which the xylem conduits serve exclusively for the transportation of sap and not also as structural elements. They argued that the metabolic cost of blood (which scales

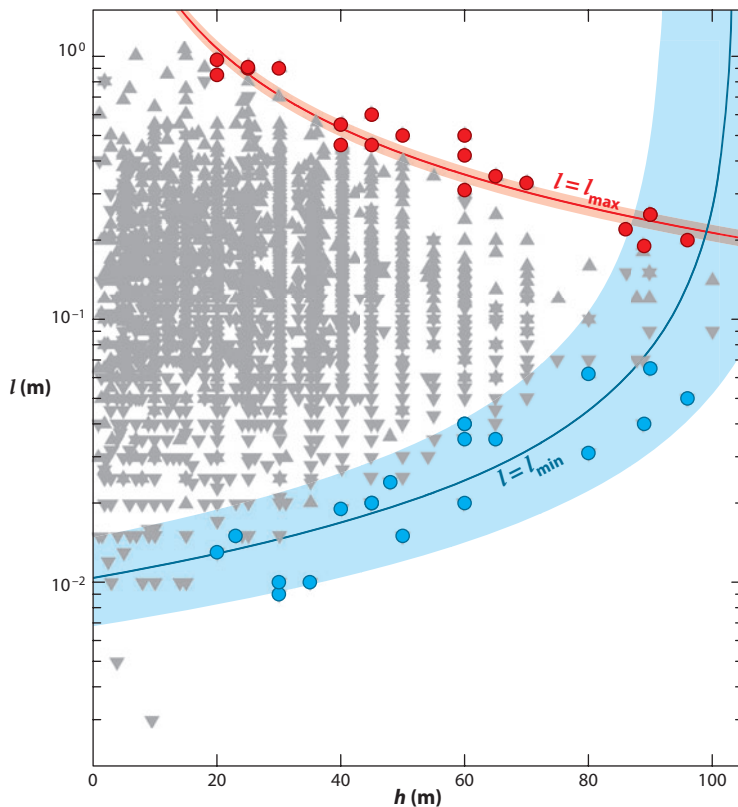


Figure 9

Scaling of leaf length with tree height. Variation in leaf size l (m) with tree height h (m) based on botanical data covering 1,925 species from 327 genera and 93 families. Gray triangles show the longest and shortest leaf lengths as a function of tree height h . Circles show the five longest (red, dark gray) and five shortest (blue, light gray) leaves in each 20-m height bin for trees taller than $h > 20$ m. Solid lines are fits for the upper bound of leaf length (l_{\max}) and lower bound of leaf length (l_{\min}) with two parameters corresponding to a minimum flow speed in the phloem [$100 (\mu\text{m s}^{-1})$] and energy output efficiency (90%). Colored fields indicate 95% confidence intervals. Figure adapted with permission from Jensen & Zwieniecki (2013).

with the vessel volume) from Murray's original argument should be replaced with the cost of synthesizing and maintaining the xylem wall in plants. A previous study showed that the volume of wall tissue scales similar to the volume of the vessel in the xylem that must resist collapse owing to reduced pressure in the sap (Hacke et al. 2001). In an argument based on the Münch hypothesis of phloem function (Section 3.2), Jensen & Zwieniecki (2013) recently showed that they could rationalize the observed upper and lower bounds of leaf length as a function of plant height (Figure 9). In an analysis based on the rate of transfer of metabolic energy through the phloem, the leaf length l (m) enters in the resistance to the flow of water into the loading zones ($R_{X-p} \sim 1/l$; Section 3.2), and height enters in the resistance to the flow of sap through the sieve tubes ($R_p \sim h$; Section 3.2). For a given height, the predicted maximum leaf length is set by the condition $R_{X-p} \ll R_p$ such that any further increase in length has little impact of the total resistance ($R_{p,\text{tot}}$; Section 3.2); this transition occurs for shorter leaf lengths in taller trees (Figure 9).

7. SYNTHETIC MIMICS OF TRANSPORT PROCESSES IN PLANTS

Synthetic systems designed to mimic the transport processes in plants have played a role in the testing of hypotheses back to at least the originators of the CT theory. In 1895, Dixon & Joly (1895) reported on an experiment in which they created a complete model of the xylem. They attached porous cups at either end of a tube and filled the entire volume with water. They then buried one cup in soil (the root) and left the other exposed to air (the leaf) and allowed the system to transpire for 8 days. Upon uncovering the root, they noted that it was noticeably warmer than the leaf. They concluded that stress generated in the leaf was transmitted via the column of liquid to the root, where it drove condensation from the vapor in the soil, in agreement with the CT theory that they and others were proposing. A year later, Askenazy described an experiment in which he sealed a porous ceramic cup filled with water to a mercury manometer (Palladin & Livingston 1926). As evaporation proceeded from the cup, the mercury rose 82 cm (liquid pressure of -7.9×10^{-3} MPa) before cavitation occurred; he concluded that the tensile strength of liquid water could be exploited in a transpiration mechanism. Through the early part of the twentieth century, scientists attempted to perfect Askenazy's experiment to generate tensions of the magnitude that CT theory implies at the tops of taller trees. In 1928, Thut (1928) reported a breakthrough based on coating a ceramic cup with a gelatin hydrogel. With this composite membrane, he reached -0.2 MPa and had more reliable results than with the uncoated ceramic membranes. Münch (1930) also developed an experiment to test his theory: He filled two osmotic bulbs with aqueous solutions of different concentrations, connected them with a liquid-filled tube, and submerged them in a bath of pure water. He noted flow from the bulb with the higher concentration to that with the lower concentration, capturing the osmotic pumping proposed in his model. Decades later, more sophisticated macromodels of phloem transport were tested (Eschrich et al. 1972, Lang 1973). Notably, Eschrich et al. (1972) created a system in which bidirectional flow was achieved, with a flow of pure fluid running outside of a tube carrying the solution; the two flow paths were coupled via osmotic membranes at their two ends.

The development of methods to create microfluidic structures (Stone et al. 2004) has provided an opportunity to revisit the challenge of forming synthetic mimics of plant vasculature. Many groups have used capillary pumping to drive flows in microfluidic systems (Effenhauser et al. 2002, Goedecke et al. 2002, Juncker et al. 2002, Guan et al. 2006). Eijkel & van den Berg (2005) pointed out that evaporation-driven flows from the ends of channels could be viewed as a form of transpiration and modeled in terms of the water potential. Working in nanochannels, Tas and colleagues inferred the existence of tension within a confined droplet of water (Tas et al. 2003) and subsequently measured tensions down to -1.5 MPa with the deflection of the channel walls (Tas et al. 2010). Also in nanochannels, Duan et al. (2012) observed the cavitation of liquid water during drying. Noblin et al. (2008) moved closer to the physiology of a leaf by forming microchannels in a silicone polymer and allowing evaporation to occur across this membrane. They used these pervaporation experiments to argue that the scaling of diffusive transport might explain the observation that, across species, the spacing between the terminal veins in leaves tends to grow linearly with the thickness of the leaf. Wheeler & Stroock (2008) formed a complete model of the xylem in the spirit of Dixon & Joly (1895), with zones representing both a leaf and a root. In the root and the leaf, they used a dense, synthetic hydrogel as a membrane material. They found that this "synthetic tree" could transpire at steady state with leaf pressures down to -1 MPa without a membrane covering the root and down to -7 MPa with a root membrane in place. Based on these observations, they concluded that (a) hydrogel-like materials may play an important role in the structure of membranes in plants, as also suggested by the experiments of Thut (1928); (b) the filtration of sap provided by the root membrane may eliminate nucleation

sites and raise the stability limit within the xylem; and (c) the tensions observed in plants (**Figures 2** and **7**) are compatible with those achievable by purely physical means. Vincent et al. (2012) recently used such a hydrogel membrane to study the dynamics of cavitation in confined volumes.

Many groups have also used osmotic mechanisms to drive flows in microfluidic systems (Eijkel et al. 2005, Velten et al. 2006, Good et al. 2007, Xu et al. 2010). Jensen et al. (2009, 2011) appear to be the first to have connected this strategy to the Münch hypothesis. Their system couples a microchannel with a flow of pure water through an osmotic membrane to a microchannel with a flow of aqueous solution. They have exploited this system to validate scaling relations between the optimal length of the sugar-loading zone and the length and diameter of the sieve tube (Jensen et al. 2011).

8. OPEN QUESTIONS AND OPPORTUNITIES

As we hope this review conveys, our understanding of the vascular physiology of plants has progressed dramatically over the past century. The development of new measurement techniques has allowed for the validation of the general features of the CT theory and the Münch hypothesis; new imaging techniques have provided views into the structure and dynamics involved in transport processes; and refinements of transport models have allowed for the elucidation of some robust rules of vascular design. Nonetheless, numerous uncertainties remain about both basic physical properties and complex biological mechanisms. The chemical composition, molecular structure, and even the conductance of many membranes in the phloem and xylem remain unknown; the means by which active biological processes intervene in the control of transport continue to emerge; and the molecular biological mechanisms (e.g., genetic regulation) that underpin vascular development and function have only just begun to be accessible in the woody species that present the most-intriguing transport processes. There are many important opportunities for impact in this field. First, there is a desire to create sensors of chemical and physical parameters to provide real-time measurements *in vivo*, for which the progression of MEMS technologies provides one route toward this goal. Second, advances in fluorescence microscopy and X-ray tomography suggest that we may be near the development of imaging tools that would allow for the visualization of structure and dynamics on the micrometer scale. Third, the tools of modern biology should be applied to elucidate the molecular origins of vascular traits and responses, with the release of whole genome sequences of woody species facilitating this development. Finally, there is a need to develop multiscale models—from the genome through the tissue to the whole plant—with which to synthesize theoretical and experimental knowledge; the progress on this type of model in human biology provides a basis for such developments for plants. These goals provide a context in which fluid mechanics couples to a rich array of physical, biological, and technical challenges.

We finish by posing the question, if plants can do it, why don't we? Why do human technologies not use liquids under tension? If we did, we would gain access to an unexploited part of the phase diagram that allows the liquid state to coexist with subsaturated phases. Manipulating liquids under tension could open new approaches in heat transfer (e.g., in heat pipes), water extraction and purification, and the manipulation of the mechanical properties of materials. Why do humans not exploit differences in osmolality to manage local differences in pressure within materials and transport systems? If we did, we could design new classes of mechanically active materials (think of a Venus fly trap) and integrate passive flow control with chemical processes. Access to these opportunities depends on the invention of new designs, materials, and manufacturing technologies informed by continued progress in the understanding of plant physiology. What could be the

inspiration? It is the plant right outside your window, serenely pumping, pulling, cavitating, and recondensing liquids as it reaches up toward the sky.

DISCLOSURE STATEMENT

The authors are not aware of any biases that might be perceived as affecting the objectivity of this review.

ACKNOWLEDGMENTS

We would like to acknowledge helpful discussions with Alan Lakso, Robert Turgeon, Jean Comtet, and Kaare Jensen during the preparation of this review. All authors acknowledge support from the Air Force Office of Scientific Research (FA9550-09-1-0188). A.D.S. and V.V.P. acknowledge support from the United States Department of Agriculture (NYG-632531). M.A.Z. and N.M.H. acknowledge support from the National Science Foundation (IOS-0919729 for M.A.Z. and IOS-1021779 and DMR-0820484 for N.M.H.).

LITERATURE CITED

- Ambrose AR, Sillett SC, Koch GW, Van Pelt R, Antoine ME, Dawson TE. 2010. Effects of height on treetop transpiration and stomatal conductance in coast redwood (*Sequoia sempervirens*). *Tree Physiol.* 30:1260–72
- Askenasy E. 1895. Ueber das Saftsteigen. *Verb. Nat. Med. Ver. Heidelb.* 5:325–45
- Azouzi ME, Ramboz C, Lenain JF, Caupin F. 2013. A coherent picture of water at extreme negative pressure. *Nat. Phys.* 9:38–41
- Boehm J. 1893. Capillarität und Saftsteigen. *Ber. Deut. Botan. Ges.* 11:203–12
- Bowen WR, Jenner F. 1995. Electroviscous effects in charged capillaries. *J. Colloid Interface Sci.* 173:388–95
- Brodersen CR, McElrone AJ, Choat B, Matthews MA, Shackel KA. 2010. The dynamics of embolism repair in xylem: in vivo visualizations using high-resolution computed tomography. *Plant Physiol.* 154:1088–95
- Canny MJ. 1995a. A new theory for the ascent of sap: cohesion supported by tissue pressure. *Ann. Bot.* 75:343–57
- Canny MJ. 1995b. Potassium cycling in helianthus: ions of the xylem sap and secondary vessel formation. *Philos. Trans. R. Soc. Lond. B* 348:457–69
- Canny MJ. 1997. Vessel contents during transpiration: embolisms and refilling. *Am. J. Bot.* 84:1223–30
- Choat B, Jansen S, Brodribb TJ, Cochard H, Delzon S, et al. 2012. Global convergence in the vulnerability of forests to drought. *Nature* 491:752–56
- Cochard H, Cruziat P, Tyree MT. 1992. Use of positive pressures to establish vulnerability curves: further support for the air-seeding hypothesis and implications for pressure-volume analysis. *Plant Physiol.* 100:205–9
- Cowan IR. 1972. Oscillations in stomatal conductance and plant functioning associated with stomatal conductance: observations and a model. *Planta* 106:185–219
- Cramer MD. 2012. Unravelling the limits to tree height: a major role for water and nutrient trade-offs. *Oecologia* 169:61–72
- Debenedetti PG. 1996. *Metastable Liquids*. Princeton, NJ: Princeton Univ. Press
- de Gennes PG, Brochard-Wyart F, Quéré D. 2004. *Capillarity and Wetting Phenomena: Drops, Bubbles, Pearls, Waves*. New York: Springer
- Dixon HH, Joly J. 1895. On the ascent of sap. *Philos. Trans. R. Soc. Lond. B* 186:563–76
- Domec JC, Lachenbruch B, Meinzer FC, Woodruff DR, Warren JM, McCulloh KA. 2008. Maximum height in a conifer is associated with conflicting requirements for xylem design. *Proc. Natl. Acad. Sci. USA* 105:12069–74
- Domec JC, Meinzer FC, Lachenbruch B, Housset J. 2007. Dynamic variation in sapwood specific conductivity in six woody species. *Tree Physiol.* 27:1389–400

- Duan C, Karnik R, Lu MC, Majumdar A. 2012. Evaporation-induced cavitation in nanofluidic channels. *Proc. Natl. Acad. Sci. USA* 109:3688–93
- Effenhäuser CS, Harttig H, Kramer P. 2002. An evaporation-based disposable micropump concept for continuous monitoring applications. *Biomed. Microdevices* 4:27–32
- Eijkel JCT, Bomer JG, van den Berg A. 2005. Osmosis and pervaporation in polyimide submicron microfluidic channel structures. *Appl. Phys. Lett.* 87:114103
- Eijkel JCT, van den Berg A. 2005. Water in micro- and nanofluidics systems described using the water potential. *Lab Chip* 5:1202–9
- Eschrich W, Evert RF, Young JH. 1972. Solution flow in tubular semipermeable membranes. *Planta* 107:279–300
- Farquhar GD, Cowan IR. 1974. Oscillations in stomatal conductance: influence of environmental gain. *Plant Physiol.* 54:769–72
- Fisher JB, Angeles G, Ewers FW, López-Portillo J. 1997. Survey of root pressure in tropical vines and woody species. *Int. J. Plant Sci.* 158:44–50
- Fu QS, Cheng LL, Guo YD, Turgeon R. 2011. Phloem loading strategies and water relations in trees and herbaceous plants. *Plant Physiol.* 157:1518–27
- Giaquinta RT. 1983. Phloem loading of sucrose. *Annu. Rev. Plant Physiol.* 34:347–87
- Goedecke N, Eijkel J, Manz A. 2002. Evaporation driven pumping for chromatography application. *Lab Chip* 2:219–23
- Goeschl JD, Magnuson CE, Demichele DW, Sharpe PJH. 1976. Concentration-dependent unloading as a necessary assumption for a closed form mathematical model of osmotically driven pressure flow in phloem. *Plant Physiol.* 58:556–62
- Good BT, Bowman CN, Davis RH. 2007. A water-activated pump for portable microfluidic applications. *J. Colloid Interface Sci.* 305:239–49
- Gouin H. 2008. A new approach for the limit to tree height using a liquid nanolayer model. *Contin. Mech. Thermodyn.* 20:317–29
- Guan YX, Xu ZR, Dai J, Fang ZL. 2006. The use of a micropump based on capillary and evaporation effects in a microfluidic flow injection chemiluminescence system. *Talanta* 68:1384–89
- Hacke UG, Sperry JS. 2003. Limits to xylem refilling under negative pressure in *Laurus nobilis* and *Acer negundo*. *Plant Cell Environ.* 26:303–11
- Hacke UG, Sperry JS, Pockman WT, Davis SD, McCulloch KA. 2001. Trends in wood density and structure are linked to prevention of xylem implosion by negative pressure. *Oecologia* 126:457–61
- Hartt CE, Kortschak HP. 1967. Translocation of ^{14}C in the sugarcane plant during the day and night. *Plant Physiol.* 42:89–94
- Herbert E, Caupin F. 2005. The limit of metastability of water under tension: theories and experiments. *J. Phys. Condens. Matter* 17:S3597–602
- Holbrook NM, Ahrens ET, Burns MJ, Zwieniecki MA. 2001. In vivo observation of cavitation and embolism repair using magnetic resonance imaging. *Plant Physiol.* 126:27–31
- Holbrook NM, Burns MJ, Field CB. 1995. Negative xylem pressures in plants: a test of the balancing pressure technique. *Science* 270:1193–94
- Holbrook NM, Zwieniecki MA. 1999. Embolism repair and xylem tension: Do we need a miracle? *Plant Physiol.* 120:7–10
- Holbrook NM, Zwieniecki MA, eds. 2005. *Vascular Transport in Plants*. Amsterdam: Elsevier
- Horwitz L. 1958. Some simplified mathematical treatments of translocation in plants. *Plant Physiol.* 33:81–93
- Jensen KH, Lee J, Bohr T, Bruus H. 2009. Osmotically driven flows in microchannels separated by a semipermeable membrane. *Lab Chip* 9:2093–99
- Jensen KH, Lee J, Bohr T, Bruus H, Holbrook NM, Zwieniecki MA. 2011. Optimality of the Münch mechanism for translocation of sugars in plants. *J. R. Soc. Interface* 8:1155–65
- Jensen KH, Berg-Sørensen K, Friis SMM, Bohr T. 2012. Analytic solutions and universal properties of sugar loading models in Münch phloem flow. *J. Theor. Biol.* 304:286–96
- Jensen KH, Zwieniecki MA. 2013. Physical limits to leaf size in tall trees. *Phys. Rev. Lett.* 110:018104
- Juncker D, Schmid H, Drechsler U, Wolf H, Wolf M, et al. 2002. Autonomous microfluidic capillary system. *Anal. Chem.* 74:6139–44

- Knoblauch M, Oparka K. 2012. The structure of the phloem: still more questions than answers. *Plant J.* 70:147–56
- Knoblauch M, Peters WS. 2010. Münch, morphology, microfluidics: our structural problem with the phloem. *Plant Cell Environ.* 33:1439–52
- Konrad W, Roth-Nebelsick A. 2003. The dynamics of gas bubbles in conduits of vascular plants and implications for embolism repair. *J. Theor. Biol.* 224:43–61
- LaBarbera M. 1990. Principles of design of fluid transport systems in zoology. *Science* 249:992–1000
- Lahey RT. 1992. *Boiling Heat Transfer: Modern Developments and Advances*. Amsterdam: Elsevier
- Lang A. 1973. Working model of a sieve tube. *J. Exp. Bot.* 24:896–904
- Lee JN, Holbrook NM, Zwieniecki MA. 2012. Ion induced changes in the structure of bordered pit membranes. *Front. Plant Sci.* 3:55
- Levich V. 1962. *Physicochemical Hydrodynamics*. Upper Saddle River, NJ: Prentice Hall
- Lewis AM, Harnden VD, Tyree MT. 1994. Collapse of water-stress emboli in the tracheids of *Thuja occidentalis* L. *Plant Physiol.* 106:1639–46
- López-Portillo J, Ewers FW, Angeles G. 2005. Sap salinity effects on xylem conductivity in two mangrove species. *Plant Cell Environ.* 28:1285–92
- Lowell S, Shields JE. 1991. *Powder Surface Area and Porosity*. New York: Chapman & Hall
- Marenco RA, Siebke K, Farquhar GD, Ball MC. 2006. Hydraulically based stomatal oscillations and stomatal patchiness in *Gossypium hirsutum*. *Funct. Plant Biol.* 33:1103–13
- McCabe WL, Smith J, Harriott P. 2005. *Unit Operations of Chemical Engineering*. New York: McGraw-Hill
- McCulloh KA, Sperry JS, Adler FR. 2004. Murray's law and the hydraulic versus mechanical functioning of wood. *Funct. Ecol.* 18:931–38
- Melcher PJ, Meinzer FC, Yount DE, Goldstein G, Zimmermann U. 1998. Comparative measurements of xylem pressure in transpiring and non-transpiring leaves by means of the pressure chamber and the xylem pressure probe. *J. Exp. Bot.* 49:1757–60
- Milburn JA. 1996. Sap ascent in vascular plants: Challengers to the cohesion theory ignore the significance of immature xylem and the recycling of Münch water. *Ann. Bot.* 78:399–407
- Milburn JA, Johnson RPC. 1966. The conduction of sap II. Detection of vibrations produced by sap cavitation in *Ricinus* xylem. *Planta* 69:43–52
- Münch E. 1930. *Die Stoffbewegungen in der Pflanze*. Jena, Ger.: Fischer
- Murray CD. 1926. The physiological principle of minimum work: I. The vascular system and the cost of blood volume. *Proc. Natl. Acad. Sci. USA* 12:207–14
- Nardini A, Gasco A, Trifilo P, Lo Gullo MA, Salleo S. 2007. Ion-mediated enhancement of xylem hydraulic conductivity is not always suppressed by the presence of Ca²⁺ in the sap. *J. Exp. Bot.* 58:2609–15
- Nardini A, Lo Gullo MA, Salleo S. 2011. Refilling embolized xylem conduits: Is it a matter of phloem unloading? *Plant Sci.* 180:604–11
- Netting AG. 2009. Limitations within “the limits to tree height.” *Am. J. Bot.* 96:542–44
- Niklas KJ. 1994. *Plant Allometry: The Scaling of Form and Process*. Chicago: Univ. Chicago Press
- Nobel PS. 1999. *Physicochemical and Environmental Plant Physiology*. San Diego: Academic
- Noblin X, Mahadevan L, Coomaraswamy IA, Weitz DA, Holbrook NM, Zwieniecki MA. 2008. Optimal vein density in artificial and real leaves. *Proc. Natl. Acad. Sci. USA* 105:9140–44
- Palladin VI, Livingston BE. 1926. *Palladin's Plant Physiology*. Boston: P. Blakiston's Son
- Philipp A, Lauterborn W. 1998. Cavitation erosion by single laser-produced bubbles. *J. Fluid Mech.* 361:75–116
- Pickard WF. 1981. The ascent of sap in plants. *Prog. Biophys. Mol. Biol.* 37:181–229
- Probststein RF. 1994. *Physicochemical Hydrodynamics: An Introduction*. New York: Wiley
- Rand RH. 1983. Fluid mechanics of green plants. *Annu. Rev. Fluid Mech.* 15:29–45
- Ryan MG, Yoder BJ. 1997. Hydraulic limits to tree height and tree growth. *Bioscience* 47:235–42
- Salleo S, Lo Gullo MA. 1989. Xylem cavitation in nodes and internodes of *Vitis vinifera* L. plants subjected to water stress: limits of restoration of water conduction in cavitated xylem conduits. In *Structural and Functional Responses to Environmental Stresses: Water Shortage*, ed. KH Kreeb, H Richter, TM Hynckley, pp. 33–42. The Hague: SPB Acad.

- Salleo S, Lo Gullo MA, De Paoli D, Zippo M. 1996. Xylem recovery from cavitation-induced embolism in young plants of *Laurus nobilis*: a possible mechanism. *New Phytol.* 132:47–56
- Salleo S, Lo Gullo MA, Trifilo P, Nardini A. 2004. New evidence for a role of vessel-associated cells and phloem in the rapid xylem refilling of cavitated stems of *Laurus nobilis* L. *Plant Cell Environ.* 27:1065–76
- Salleo S, Trifilo P, Esposito S, Nardini A, Lo Gullo MA. 2009. Starch-to-sugar conversion in wood parenchyma of field-growing *Laurus nobilis* plants: a component of the signal pathway for embolism repair? *Funct. Plant Biol.* 36:815–25
- Scholander PF, Bradstreet ED, Hemmingsen EA, Hammel HT. 1965. Sap pressure in vascular plants: Negative hydrostatic pressure can be measured in plants. *Science* 148:339–46
- Secchi F, Gilbert ME, Zwieniecki MA. 2011. Transcriptome response to embolism formation in stems of *Populus trichocarpa* provides insight into signaling and the biology of refilling. *Plant Physiol.* 157:1419–29
- Secchi F, Zwieniecki MA. 2010. Patterns of PIP gene expression in *Populus trichocarpa* during recovery from xylem embolism suggest a major role for the PIP1 aquaporin subfamily as moderators of refilling process. *Plant Cell Environ.* 33:1285–97
- Secchi F, Zwieniecki MA. 2011. Sensing embolism in xylem vessels: the role of sucrose as a trigger for refilling. *Plant Cell Environ.* 34:514–24
- Slatyer RO. 1967. *Plant-Water Relationships*. London: Academic
- Smith JAC, Milburn JA. 1980. Phloem turgor and the regulation of sucrose loading in *Ricinus communis* L. *Planta* 148:42–48
- Sperry JS. 2003. Evolution of water transport and xylem structure. *Int. J. Plant Sci.* 164:S115–27
- Stone HA, Stroock AD, Ajdari A. 2004. Engineering flows in small devices: microfluidics toward a lab-on-a-chip. *Annu. Rev. Fluid Mech.* 36:381–411
- Taiz L, Zeiger E. 2010. *Plant Physiology*. Sunderland, MA: Sinauer Assoc.
- Tas NR, Escalante M, van Honschoten JW, Jansen HV, Elwenspoek M. 2010. Capillary negative pressure measured by nanochannel collapse. *Langmuir* 26:1473–76
- Tas NR, Mela P, Kramer T, Berenschot JW, van den Berg A. 2003. Capillarity induced negative pressure of water plugs in nanochannels. *Nano Lett.* 3:1537–40
- Thompson MV. 2006. Phloem: the long and the short of it. *Trends Plant Sci.* 11:26–32
- Thompson MV, Holbrook NM. 2003. Scaling phloem transport: water potential equilibrium and osmoregulatory flow. *Plant Cell Environ.* 26:1561–77
- Thut HF. 1928. Demonstrating the lifting power of transpiration. *Ohio J. Sci.* 28:292–98
- Turgeon R. 2010a. The puzzle of phloem pressure. *Plant Physiol.* 154:578–81
- Turgeon R. 2010b. The role of phloem loading reconsidered. *Plant Physiol.* 152:1817–23
- Tyree MT, Dixon MA. 1983. Cavitation events in *Thuja occidentalis* L: Ultrasonic acoustic emissions from the sapwood can be measured. *Plant Physiol.* 72:1094–99
- Tyree MT, Salleo S, Nardini A, Lo Gullo MA, Mosca R. 1999. Refilling of embolized vessels in young stems of laurel: Do we need a new paradigm? *Plant Physiol.* 120:11–21
- Tyree MT, Sperry JS. 1989. Vulnerability of xylem to cavitation and embolism. *Annu. Rev. Plant Physiol. Plant Mol. Biol.* 40:19–38
- Tyree MT, Yang SD. 1992. Hydraulic conductivity recovery versus water pressure in xylem of *Acer saccharum*. *Plant Physiol.* 100:669–76
- Tyree MT, Zimmermann MH. 1971. The theory and practice of measuring transport coefficients and sap flow in the xylem of red maple stems (*Acer rubrum*). *J. Exp. Biol.* 70:1–18
- Tyree MT, Zimmermann MH. 2002. *Xylem Structure and the Ascent of Sap*. Berlin: Springer-Verlag
- van Doorn WG, Hiemstra T, Fanourakis D. 2011. Hydrogel regulation of xylem water flow: an alternative hypothesis. *Plant Physiol.* 157:1642–49
- van Ieperen W, van Meeteren U, van Gelder H. 2000. Fluid ionic composition influences hydraulic conductance of xylem conduits. *J. Exp. Bot.* 51:769–76
- Velten T, Schuck H, Knoll T, Scholz O, Schumacher A, et al. 2006. Intelligent intraoral drug delivery microsystem. *Proc. Inst. Mech. Eng. C* 220:1609–17
- Vincent O, Marmottant P, Quinto-Su PA, Ohl CD. 2012. Birth and growth of cavitation bubbles within water under tension confined in a simple synthetic tree. *Phys. Rev. Lett.* 108:184502

- Wheeler TD, Stroock AD. 2008. The transpiration of water at negative pressures in a synthetic tree. *Nature* 455:208–12
- Wheeler TD, Stroock AD. 2009. Stability limit of liquid water in metastable equilibrium with subsaturated vapors. *Langmuir* 25:7609–22
- Woodruff DR, Bond BJ, Meinzer FC. 2004. Does turgor limit growth in tall trees? *Plant Cell Environ.* 27:229–36
- Xu ZR, Yang CG, Liu CH, Zhou Z, Fang J, Wang JH. 2010. An osmotic micro-pump integrated on a microfluidic chip for perfusion cell culture. *Talanta* 80:1088–93
- Zheng Q, Durben DJ, Wolf GH, Angell CA. 1991. Liquids at large negative pressures: water at the homogeneous nucleation limit. *Science* 254:829–32
- Zimmermann MH. 1978. Hydraulic architecture of some diffuse-porous trees. *Can. J. Bot.* 56:2286–95
- Zimmermann U, Schneider H, Wegner LH, Wagner H-J, Szimtenings M, et al. 2002. What are the driving forces for water lifting in the xylem conduit? *Physiol. Plant.* 114:327–35
- Zufferey V, Cochard H, Ameglio T, Spring JL, Viret O. 2011. Diurnal cycles of embolism formation and repair in petioles of grapevine (*Vitis vinifera* cv. Chasselas). *J. Exp. Bot.* 62:3885–94
- Zwieniecki MA, Holbrook NM. 1998. Diurnal variation in xylem hydraulic conductivity in white ash (*Fraxinus americana* L.), red maple (*Acer rubrum* L.) and red spruce (*Picea rubens* Sarg.). *Plant Cell Environ.* 21:1173–80
- Zwieniecki MA, Holbrook NM. 2000. Bordered pit structure and vessel wall surface properties: implications for embolism repair. *Plant Physiol.* 123:1015–20
- Zwieniecki MA, Holbrook NM. 2009. Confronting Maxwell's demon: biophysics of xylem embolism repair. *Trends Plant Sci.* 14:530–34
- Zwieniecki MA, Melcher PJ, Holbrook NM. 2001. Hydrogel control of xylem hydraulic resistance in plants. *Science* 291:1059–62



Contents

Taking Fluid Mechanics to the General Public <i>Etienne Guyon and Marie Yvonne Guyon</i>	1
Stably Stratified Atmospheric Boundary Layers <i>L. Mahrt</i>	23
Rheology of Adsorbed Surfactant Monolayers at Fluid Surfaces <i>D. Langevin</i>	47
Numerical Simulation of Flowing Blood Cells <i>Jonathan B. Freund</i>	67
Numerical Simulations of Flows with Moving Contact Lines <i>Yi Sui, Hang Ding, and Peter D.M. Spelt</i>	97
Yielding to Stress: Recent Developments in Viscoplastic Fluid Mechanics <i>Neil J. Balmforth, Ian A. Frigaard, and Guillaume Ovarlez</i>	121
Dynamics of Swirling Flames <i>Sébastien Candel, Daniel Durox, Thierry Schuller, Jean-François Bourgoin, and Jonas P. Moeck</i>	147
The Estuarine Circulation <i>W. Rockwell Geyer and Parker MacCready</i>	175
Particle-Resolved Direct Numerical Simulation for Gas-Solid Flow Model Development <i>Sudbeer Tenneti and Shankar Subramaniam</i>	199
Internal Wave Breaking and Dissipation Mechanisms on the Continental Slope/Shelf <i>Kevin G. Lamb</i>	231
The Fluid Mechanics of Carbon Dioxide Sequestration <i>Herbert E. Huppert and Jerome A. Neufeld</i>	255
Wake Signature Detection <i>Geoffrey R. Spedding</i>	273
Fast Pressure-Sensitive Paint for Flow and Acoustic Diagnostics <i>James W. Gregory, Hirotaka Sakaue, Tianshu Liu, and John P. Sullivan</i>	303

Instabilities in Viscosity-Stratified Flow <i>Rama Govindarajan and Kirti Chandra Sabu</i>	331
Water Entry of Projectiles <i>Tadd T. Truscott, Brenden P. Epps, and Jesse Belden</i>	355
Surface Acoustic Wave Microfluidics <i>Leslie Y. Yeo and James R. Friend</i>	379
Particle Transport in Therapeutic Magnetic Fields <i>Isbwar K. Puri and Ranjan Ganguly</i>	407
Aerodynamics of Heavy Vehicles <i>Haecheon Choi, Jungil Lee, and Hyungmin Park</i>	441
Low-Frequency Unsteadiness of Shock Wave/Turbulent Boundary Layer Interactions <i>Noel T. Clemens and Venkateswaran Narayanaswamy</i>	469
Adjoint Equations in Stability Analysis <i>Paolo Luchini and Alessandro Bottaro</i>	493
Optimization in Cardiovascular Modeling <i>Alison L. Marsden</i>	519
The Fluid Dynamics of Competitive Swimming <i>Timothy Wei, Russell Mark, and Sean Hutchison</i>	547
Interfacial Layers Between Regions of Different Turbulence Intensity <i>Carlos B. da Silva, Julian C.R. Hunt, Ian Eames, and Jerry Westerweel</i>	567
Fluid Mechanics, Arterial Disease, and Gene Expression <i>John M. Tarbell, Zhong-Dong Shi, Jessilyn Dunn, and Hanjoong Jo</i>	591
The Physicochemical Hydrodynamics of Vascular Plants <i>Abraham D. Stroock, Vinay V. Pagay, Maciej A. Zwieniecki, and N. Michele Holbrook</i>	615

Indexes

Cumulative Index of Contributing Authors, Volumes 1–46	643
Cumulative Index of Article Titles, Volumes 1–46	652

Errata

An online log of corrections to *Annual Review of Fluid Mechanics* articles may be found at <http://fluid.annualreviews.org/errata.shtml>